

**Integrating Low-cost Air Quality Monitoring Sensors with
Solar Power System and Emissions Assessment of 2022 Fire
Events in Islamabad Capital Territory (ICT)**



By

Nameer Urfi

(Registration No: 00000328014)

Institute of Environmental Sciences and Engineering

School of Civil and Environmental Engineering

National University of Sciences & Technology (NUST)

Islamabad, Pakistan

(2024)

**Integrating Low-cost Air Quality Monitoring Sensors with
Solar Power System and Emissions Assessment of 2022 Fire
Events in Islamabad Capital Territory (ICT)**



By

Nameer Urfi

(Registration No: 00000328014)

A thesis submitted to the National University of Sciences and Technology, Islamabad,

in partial fulfillment of the requirements for the degree of

Master of Science in
Environmental Sciences

Supervisor: Dr. Muhammad Fahim Khokhar

School of Civil and Environmental Engineering

National University of Sciences & Technology (NUST)

Islamabad, Pakistan

(2024)

THESIS ACCEPTANCE CERTIFICATE

It is certified that the final copy of the MS/MPhil Thesis written by Mr. Nansoor Urfi (Registration No: 00000328014) of SCEE (IESE) has been vetted by the undersigned, found complete in all respects as per NUST Statutes/Regulations, is free of plagiarism, errors, and mistakes, and is accepted as partial fulfillment for the award of MS/MPhil degree. It is further certified that necessary amendments as pointed out by GEC members of the scholar have also been incorporated in the said thesis.

Signature: _____

Name of Supervisor: Dr Muhammad
Fahim Khokhar

Date: 10.09.2024

Dr. Zeshan
Tenured Professor
HoD Environmental Sciences
SCEE (IESE) NUST Islamabad

Signature (HOD): _____

Date: 15/11/2024

Signature (Associate Dean): _____

PROF DR MUHAMMAD ARSHAD
Associate Dean SCEE (IESE)
NUST H-12, Islamabad

Date: 18.11.2024

Signature (Principal & Dean SCEE): _____

PROF DR MUHAMMAD IRFAN
Principal & Dean
SCEE, NUST

Date: 28 NOV 2024

CERTIFICATE OF APPROVAL

This is to certify that the research work presented in this thesis, entitled "Integrating Low-Cost Air Quality Monitoring Sensors with Solar Power System and Emissions Assessment of 2022 Fire Events in Islamabad Capital Territory (ICT)" was conducted by Mr. Nameer Urfi under the supervision of Dr. Muhammad Fahim Khokhar.

No part of this thesis has been submitted anywhere else for any other degree. This thesis is submitted to SCEE (IESE) in partial fulfillment of the requirements for the degree of Master of Science in the field of Environmental Sciences.

School of Civil and Environmental Engineering, National University of Sciences and Technology, Islamabad.

Student Name: **Nameer Urfi**

Signature: _____

Guidance and Examination Committee:

a) **Dr. Muhammad Arshad**
Professor, SCEE (IESE)

Signature: _____

b) **Dr. Rashid Inakhar**
Assistant Professor, SCEE (IESE)

Signature: _____

Supervisor: **Dr Muhammad Fahim Khokhar**
Professor
SCEE (IESE)

Signature: _____

HOD: **Dr. Zeshan**

Dr. Zeshan
Tenured Professor
HoD Environmental Sciences
SCEE (IESE) NUST Islamabad

Signature: _____

Associate Dean: **Dr Muhammad Arshad**

PROF DR MUHAMMAD ARSHAD
Associate Dean SCEE (IESE)
NUST H-12, Islamabad

Signature: _____


Principal & Dean SCEE

Signature: _____

PROF DR MUHAMMAD IRFAN
Principal & Dean
SCEE, NUST

AUTHOR'S DECLARATION CERTIFICATE

I, Nameer Urfi hereby state that my MS thesis titled "Integrating Low-Cost Air Quality Monitoring Sensors with Solar Power System and Emissions Assessment of 2022 Fire Events in Islamabad Capital Territory (ICT)" is my own work and has not been submitted previously by me for taking any degree from National University of Sciences and Technology, Islamabad or anywhere else in the country/ world. At any time if my statement is found to be incorrect even after I graduate, the university has the right to withdraw my MS degree.

Student Signature:  _____

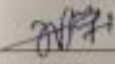
Name: Nameer Urfi

PLAGIARISM UNDERTAKING

I solemnly declare that research work presented in the thesis titled "Integrating Low-Cost Air Quality Monitoring Sensors with Solar Power System and Emissions Assessment of 2022 Fire Events in Islamabad Capital Territory (ICT)" is solely my research work with no significant contribution from any other person. Small contribution/help wherever taken has been duly acknowledged and that complete thesis has been written by me.

I understand the zero-tolerance policy of the HEC and National University of Sciences and Technology (NUST), Islamabad towards plagiarism. Therefore, I as an author of the above titled thesis declare that no portion of my thesis has been plagiarized and any material used as reference is properly referred/cited.

I undertake that if I am found guilty of any formal plagiarism in the above titled thesis even after award of MS degree, the University reserves the rights to withdraw/ revoke my MS degree and that HEC and NUST, Islamabad has the right to publish my name on the HEC/University website on which names of students are placed who submitted plagiarized thesis.

Student's Signature: 

Student's Name: Nameer Urfi

Date: 10.09.2024

DEDICATION

I dedicate this thesis to my Beloved Prophet Muhammad ﷺ who has forever been my guide and source of inspiration in every aspect of my life.

ACKNOWLEDGEMENTS

Praise be to the highest God for the magnificent deeds accomplished. I express my profound gratitude for the abundant provisions, protections, and guidance bestowed upon me throughout this endeavor. Foremost, I attribute the completion of this manuscript to the grace of Almighty Allah. I hold utmost reverence for Prophet Muhammad ﷺ, whose exemplary life serves as the cornerstone of my own.

I am deeply appreciative of my supervisor, Dr. Muhammad Fahim Khokhar (IESE), for his discerning feedback, constructive criticism, and unwavering encouragement. I am indebted to him for dedicating his valuable time to departmental discussions and offering concrete suggestions to enhance both the research and thesis composition.

I extend my heartfelt thanks to the members of the committee, Dr. Muhammad Arshad (IESE) and Dr. Rashid Iftikhar (IESE), for graciously allocating time from their busy schedules to participate in progress reviews and provide invaluable insights and feedback on the research and thesis. My gratitude also extends to the entire faculty, staff of IESE, and my peers for their steadfast support and guidance throughout the research journey.

TABLE OF CONTENTS

ACKNOWLEDGEMENTS	viii
TABLE OF CONTENTS	ix
LIST OF TABLES	xi
LIST OF FIGURES	xii
LIST OF SYMBOLS, ABBREVIATIONS AND ACRONYMS	xiii
ABSTRACT	xv
CHAPTER 1: INTRODUCTION	1
1.1 BACKGROUND:	1
<i>1.1.1 STATE OF AIR QUALITY IN PAKISTAN:</i>	2
1.2 INCEPTION OF LOW-COST AIR QUALITY MONITORING SENSORS:	3
<i>1.1.2 EXPECTED OUTCOMES OF THIS STUDY:</i>	4
1.3 OBJECTIVES:	5
	Error! Bookmark not defined.
CHAPTER 2: LITERATURE REVIEW	6
2.1 AIR POLLUTION:	6
2.2 AIR QUALITY MONITORING:	6
<i>1.2.1 PARTICULATE MATTER:</i>	7
2.3 LOW-COST AIR QUALITY MONITORING SENSORS AND NETWORKS:	8
2.4 WILDFIRES AND BUSHFIRES:	10
<i>2.4.1 FORESTS:</i>	11
<i>2.4.2 TEMPERATE FORESTS:</i>	11
<i>2.4.3 MIXED FORESTS:</i>	12
<i>2.4.4 MEDITERRANEAN FORESTS:</i>	12
<i>2.4.5 GRASSLANDS (STEPPE):</i>	12
<i>2.4.6 SCRUBLANDS:</i>	13
2.5 ABOVE-GROUND BIOMASS:	13
CHAPTER 3: METHODOLOGY	15
3.1 TSI LOW-COST AQM SENSORS:	15
<i>3.1.1 PURPOSE OF USING TSI LOW-COST SENSORS:</i>	18
<i>3.1.2 LIMITATIONS OF LOW-COST SENSORS:</i>	19
3.2 INTEGRATION WITH SOLAR PANEL:	19
<i>3.2.1 SOLAR PANEL SPECIFICATIONS:</i>	20

3.3	FINANCIAL FEASIBILITY:	22
3.4	FIRE EVENT INITIAL ASSESSMENT:	23
3.5	STUDY AREA:	24
3.6	DATA SETS:	24
3.7	BURN AREA DETECTION:	25
3.8	PRE-FIRE/POST-FIRE VISUALIZATION:	26
3.9	SYNTHETIC APERTURE RADAR (SAR) VISUALIZATION:	27
3.9.1	<i>DATA PRODUCTS OF SAR:</i>	28
3.9.2	<i>SAR DATA FOR THIS STUDY:</i>	29
3.9.3	<i>SAR Visualized Burned Area:</i>	30
3.10	NORMALIZED BURN RATIO:	31
3.11	EMISSION ESTIMATION:	32
3.11.1	<i>EMISSIONS ESTIMATION PROCESS:</i>	33
CHAPTER 4: RESULTS AND DISCUSSIONS		34
4.1	LOW-COST SENSOR NETWORK:	34
4.2	FIRE EVENT IN NUST H-12:	34
4.3	SATELLITE VS BLUESKY SENSOR OBSERVATIONS:	36
4.4	DISCUSSION:	37
4.5	ABOVE GROUND BIOMASS (AGB) / BURNT BIOMASS:	37
4.5.1	<i>BURN SEVERITY:</i>	38
4.6	EMISSION ESTIMATION:	39
4.6.1	<i>CONVERSION FACTORS:</i>	40
4.6.2	<i>EMISSIONS AT NUST:</i>	41
4.6.3	<i>EMISSIONS AT MARGALLA HILLS:</i>	42
4.6.4	<i>EMISSIONS IN KARORE VILLAGE:</i>	44
4.6.5	<i>EMISSIONS IN PATRIATA:</i>	46
CHAPTER 5: CONCLUSIONS AND FUTURE RECOMMENDATION		48
5.1	CONCLUSIONS:	48
5.2	RECOMMENDATIONS:	50
REFERENCES		51

LIST OF TABLES

	Page No.
Table 3.1 Solar panel specifications for wireless independent low-cost air quality sensor	20
Table 3.2 Conditions for first scenario for observing technical feasibility of solar power backup with low-cost sensor	21
Table 3.3 Conditions for second scenario for observing technical feasibility of solar power backup with low-cost sensor	22
Table 3.4 Financial feasibility of integrating low-cost sensor with solar power backup	23
Table 4. 1 Above-average above-ground biomass (α) and burned biomass amount (B) constants by EMEP/EEA, 2019	38
Table 4. 2 Burn severity (β) constants for forests and scrubland suggested by EMEP/EEA 2019	39
Table 4. 3 Location-wise burned area, emitted dry mass and carbon mass using biomass combustion model.....	40
Table 4. 4 Conversion factor for each pollutant as suggested by EMEP/EEA 2019	41
Table 4. 5 Concentration of each pollutant in NUST using emission factor by EMEP/EEA 2019	41
Table 4. 6 Concentration of each pollutant in Margalla Hill sites using emission factor by EMEP/EEA 2019	43
Table 4. 7 Concentration of each pollutant in Karore Village using emission factor by EMEP/EEA 2019	45
Table 4. 8 Concentration of each pollutant in Patriata using emission factor by EMEP/EEA 2019	47

LIST OF FIGURES

Page No.

Figure 1.1 Process flow diagram for methodology against Objective1. **Error! Bookmark not defined.**

Figure 1.2 Process flow diagram for methodology against Objective2. **Error! Bookmark not defined.**

Figure 3. 1 Top view (left) and bottom view (right) of TSI BlueSky Low-cost Air Quality Monitoring Sensor 17

Figure 3. 2 User interface of TSI cloud site for registering the devices online before installment. Location and type of devices are added manually. 18

Figure 3. 3 Solar integrated assembly of low-cost air quality monitoring sensor at IESE, NUST20

Figure 3. 4 Active fire points of Islamabad Capital Territory and surroundings on 8th June, 2022 25

Figure 3. 5 Sentinel 2-A 20m x 20m resolution RGB image of active fires and burned areas in and around Islamabad Capital Territory manually marked using ArcMap 10.8..... 26

Figure 3. 6 Sentinel 2-A 20m x 20m resolution RGB image of active fires and burned areas in and around Islamabad Capital Territory on 6th June, 2022 27

Figure 3. 7 Sentinel 2-A 20m x 20m resolution RGB image of active fires and burned areas in and around Islamabad Capital Territory on 8th June, 2022 27

Figure 3. 8 User interface of SNAP (Sentinel Application Platform) version 4.0.0 while processing a C-Band image from Sentinel 1-C..... 30

Figure 3. 9 Burned area at NUST H-12 Campus visualized in VV-VH C-band calibrated and corrected image of Sentinel 1-C 31

Figure 3. 10 Delta-NBR index for fire in ICT classified maximum (highest severity) to minimum (lowest severity)..... 32

Figure 4. 1 TSI BlueSky low-cost sensor network in Islamabad and Rawalpindi against the installations all over Pakistan 34

Figure 4. 2 User interface of software to observe meteorological parameters through weather station installed at IESE, NUST..... 35

Figure 4. 3 Sentinel 2-A 20m x 20m RGB image and VIIRS active fire hotspot MODIS products verifying active burning site in NUST H-12 Campus on 8th June, 2022 36

Figure 4. 4 TSI BlueSky sensors NUST Pk-3 and NUST Pk-6 installed at IESE, NUST response to fire on 7th June, 2022..... 37

Figure 4. 5 Pie-chart distribution of emitted dry mass concentration relevant to the respective location..... 40

Figure 4. 6 Pie-chart distribution of concentration of each pollutant at NUST H-12 Campus 42

Figure 4. 7 Comparison of Sentinel 2-A RGB image against VIIRS fire hotspot products against TSI BlueSky sensors’ increased concentration..... 42

Figure 4. 8 Pie-chart distribution of concentration of each pollutant at Margalla Hills..... 43

Figure 4. 9 Active burning sites around Karore village verified by VIIRS fire hotspot product and Sentinel 2-A RGB image 44

Figure 4. 10 Pie-chart distribution of concentration of each pollutant at Karore Village 45

Figure 4. 11 Active burning sites around Patriata verified by VIIRS fire hotspot product and Sentinel 2-A RGB image 46

Figure 4. 12 Pie-chart distribution of concentration of each pollutant at Patriata..... 47

LIST OF SYMBOLS, ABBREVIATIONS AND ACRONYMS

PM	Particulate Matter
LCS	Low-cost Sensor
EPA	Environment Protection Agency
NEQS	National Environment Quality Standards
AQI	Air Quality Index
WHO	World Health Organization
BC	Black Carbon
CO	Carbon Monoxide
NO _x	Oxides of Nitrogen
SO ₂	Sulphur dioxide
O ₃	Ozone
VOCs	Volatile Organic Compounds
IoT	Internet of Things
LWSN	Low-cost Wireless Sensor Network
IESE	Institute of Environmental Sciences and Engineering
NUST	National University of Science and Technology
ICT	Islamabad Capital Territory

VIIRS	Visible Infrared Imaging Radiometer Suite
NASA	National Aeronautics and Space Administration
SAR	Synthetic Aperture Radar
GRD	Ground Range Detected
SLC	Single Look Complex
ESA	European Space Agency
SNAP	Sentinel Application Platform
SRTM	Shuttle Radar Topography Mission
NBR	Normalized Burn Ratio
NIR	Near Infrared
SWIR	Shortwave Infrared
EMEP	European Monitoring and Evaluation Program
MODIS	Moderate Resolution Imaging Spectroradiometer
TSP	Total Suspended Particles
BCM	Biomass Combustion Model

ABSTRACT

Air pollution poses a significant global challenge, particularly impacting health and economic well-being. It has been identified as the 5th leading cause of human mortality (Health Effects Institute, 2019), with developing countries bearing a disproportionate burden. In 2022, the World Health Organization (WHO) reported that approximately 99 percent of the global population was exposed to unhealthy air conditions, with low and moderate-income regions being particularly affected (WHO, 2022). In regions like South Asia, deficient resources and inadequate health infrastructure exacerbate the impact of air pollution. Particulate matter, notably $PM_{2.5}$, emerges as a critical pollutant, capable of causing respiratory distress, neurological damage, and carcinogenic effects upon inhalation (Orach et al., 2021). Currently, the monitoring infrastructure is insufficient to cover all vulnerable areas in densely populated countries. Conventional monitoring instruments are expensive, require significant maintenance, and need substantial human resources to meet the sampling demands in these regions. (Chu et al., 2020). This study investigates the technical and financial feasibility of developing a single solar-integrated, low-cost sensor unit. The proposed sensor unit incorporates batteries, charge controllers, and solar panels to ensure autonomy and sustainability. This research delves into the analysis of bushfire activity within the Islamabad Capital Territory (ICT) during the summer of 2022, which also affected the NUST H-12 campus. Utilizing satellite imaging, the study examines the temporal and spatial characteristics of the fires. Furthermore, pollutant categorization, including $PM_{2.5}$, PM_{10} , nitrogen oxides, sulfur oxides, methane, black carbon, and total suspended particles, is conducted using a biomass combustion model.

Keywords: Air quality; particulate matter; bushfire; low-cost sensor; solar power

CHAPTER 1: INTRODUCTION

1.1 BACKGROUND:

Climate change and air pollution pose significant challenges in Pakistan (Manisalidis et al., 2020). The detrimental impact of air pollution on the local population's health is a matter of concern, with substantial evidence suggesting a reduction in average life expectancy (Mir et al., 2022). Notably, PM_{2.5} pollution ranks as the third leading cause of fatalities attributable to air pollution. However, Pakistan faces a dearth of comprehensive ground-level data due to a limited number of air monitoring stations (Bilal et al., 2021). Studies indicate that in 2017, the majority of Lahore's population was exposed to PM_{2.5} levels exceeding the recommended guidelines set by the World Health Organization (Chu et al., 2020). The concentration of various chemicals and hazardous pollutants in urban areas exacerbates the susceptibility of the urban population to infectious diseases. Consequently, Pakistan, being the second most urbanizing nation in South Asia, ranked as the second most polluted country globally in 2020 (Manisalidis et al., 2020). Addressing air quality issues necessitates urgent and effective measures. Presently, monitoring infrastructure is inadequate to cover all vulnerable areas in a densely populated country. Conventional monitoring instruments are not only expensive but also require substantial maintenance and human resources to meet the demand for sampling in densely populated regions. In contrast, wireless sensor-based instruments offer a promising solution, providing a wider spatial coverage and potentially overcoming the limitations of conventional methods (Chu et al., 2020).

Table 1 Pakistan Environmental Quality Standards (Pak-NEQs) (Pak-EPA, 2005) and World Health Organization (WHO Fact Sheet, 2018) ambient air standards.

	Pollutants	Pak NEQs	WHO	US EPA	
		($\mu\text{g}/\text{m}^3$)	($\mu\text{g}/\text{m}^3$)	($\mu\text{g}/\text{m}^3$)	
24-hour mean	PM ₁₀	150	45	150	
Annual Mean		120	15	50	
24-hour mean	PM _{2.5}	35	15	35	
Annual Mean		15	5	12	

1.1.1 STATE OF AIR QUALITY IN PAKISTAN:

The escalating global population growth coupled with the excessive exploitation of natural resources has heightened concerns regarding air pollution as a critical environmental issue on a worldwide scale. According to the World Health Organization (Manisalidis et al., 2020; Tainio et al., 2021), alarming levels of air pollution prevail globally, with an estimated 9 out of 10 individuals exposed to polluted air. Annually, outdoor and indoor aerosol pollutants contribute to approximately 7 million deaths. Outdoor (ambient) air pollution arises from elevated concentrations of various pollutants, including airborne particulate matter (PM), ozone (O₃), nitrogen dioxide (NO₂), volatile organic compounds (VOC), carbon monoxide (CO), and sulfur dioxide (SO₂), all of which pose significant health risks (Orach et al., 2021). Despite being a global issue, recent data from the WHO air quality database highlights that 97% of affected cities are situated in low- and middle-income countries, each with populations exceeding 100,000 inhabitants (Jiang & Bell, 2008; Manisalidis et al., 2020; Tainio et al., 2021). Pakistan, (Government of Pakistan & Ministry of Planning, 2022) categorized among the low- and middle-income nations, grapples with endemic air pollution, particularly in its urban centers. Notably, Pakistan stands as the population

among its South Asian counterparts, with an urban population of 77.42 million, constituting 36.37% of the total population, and exhibiting an annual growth rate of 2.52% (Rasheed et al., 2014).

The Health Effects Institute (2022) has documented that Pakistan's entire population has been consistently exposed to annual mean concentrations of PM_{2.5} (defined as the integrated dry mass of aerosol particulates with an aerodynamic diameter less than 2.5 µm), reaching 58 µg/m³ in 2017. These levels surpass the WHO Interim Target-1 threshold of <35 µg/m³. Pakistan ranks prominently on the global scale concerning mortality resulting from air pollution, occupying the third position worldwide, with an estimated annual toll of 128,000 lives (Rasheed et al., 2015).

Air pollutants encompass both gaseous pollutants and particulate matters (PM). The pathogenicity of PM is contingent upon various factors including size, composition, origin, solubility, and their capacity to generate reactive oxygen species. Research findings have indicated that smog typically arises from elevated concentrations of fine particles, specifically those with a size equal to or less than 2.5 µm, commonly referred to as PM_{2.5}, or aerosols. Investigations have revealed that particulate matters with an aerodynamic diameter smaller than 10 µm exert a more pronounced impact on human health. Among the identified particulate matters, PM_{2.5} stands out due to its diminutive size but substantial surface area, potentially facilitating the transport of diverse toxic substances. These particles can bypass the filtration mechanism of nasal hair, traverse the respiratory tract with airflow, and accumulate in the distal regions via diffusion, thereby causing damage to various organs through the exchange of air in the lungs (Hosseini et al., 2010; Rasheed et al., 2015).

1.2 INCEPTION OF LOW-COST AIR QUALITY MONITORING SENSORS:

Monitoring of air quality holds a great importance to achieve a significant amount of data to take policy actions. Low-cost sensors can potentially revolutionize the spatio-temporal dynamics of air quality monitoring specially in low-income countries (Sahu et al., 2020). A commendable trend among companies is the development of accessible and cost-effective devices for monitoring PM_{2.5} levels, with the emergence of low-cost sensors representing a noteworthy technological advancement. These sensors hold

versatile applications, ranging from assessing the exposure of the general populace, particularly vulnerable demographics, to identifying pollutant sources, evaluating traffic hotspots, and augmenting monitoring coverage by integrating with existing observation infrastructure (Bilgiç et al., 2021; Lin et al., 2017).

Low-cost sensors (LCS) offer compactness, ease of deployment across diverse locations, high resolution coverage, affordability compared to conventional instruments, and straightforward operability. Particularly advantageous for low- and middle-income economies grappling with limited air monitoring infrastructure, LCS mitigate the challenges posed by sparse monitoring stations. Presently, a variety of LCS from various manufacturers are readily available at reduced costs and can operate autonomously without requiring human intervention. However, despite their merits, LCS do not yet serve as a comprehensive substitute for all reference instruments due to potential limitations in data precision and accuracy, as well as weak specificity. These shortcomings could be addressed through the establishment of an extensive sensor network, enhancing the overall effectiveness and reliability of LCS-based monitoring systems. Low-cost sensors (LCSs) offer significant advantages for low and middle-income economies (Xie et al., 2015), particularly in addressing air monitoring challenges arising from limited station availability. However, these sensors are not without their shortcomings, which require resolution. One common issue is the need for frequent calibrations to maintain accuracy. To address this, recent advancements have integrated machine learning techniques along with quadratic and linear models into the calibration process (Liang, 2021).

1.1.2 EXPECTED OUTCOMES OF THIS STUDY:

This study is aimed to comprehend the utilization of low-cost air quality monitoring sensors in urban settlements to build a monitoring framework. Although low-cost sensors provide an economical and affordable solution to air quality monitoring as compared to conventional equipment, yet they come with some limitations such as power and internet supply, sensor life and replacement etc. This study is focused on devising a solution to these limitations while analyzing the case study of extreme bushfire events in Islamabad Capital Territory and surrounding areas in June 2022.

1.3 RESEARCH GAP:

The current air quality monitoring infrastructure in Pakistan is notably deficient. Existing technologies are outdated, bulky, immobile, and costly, resulting in highly localized data that fails to provide comprehensive insights necessary for city- or district-level policy decisions. In recent years, major Pakistani cities have suffered severe air pollution, particularly industrial smog during winters, adversely affecting millions of residents' health for prolonged periods. This inadequate monitoring infrastructure creates a research gap, hindering effective policy formulation and leaving mitigation measures insufficient. This study proposes the implementation of low-cost air quality sensors, which are easily deployable, user-friendly, and cost-effective. These sensors can be strategically networked across urban, semi-urban and rural areas to yield reliable data, offering a promising approach to monitor broader regions and facilitate more informed policy decisions

1.4 OBJECTIVES:

The objectives of this study are as follows:

- Technical and financial feasibility of transforming low-cost sensor on solar power
- Assessment of emissions of pollutants during wildfire activity around Islamabad Capital Territory in May-June, 2022 using Biomass Combustion Model.

CHAPTER 2: LITERATURE REVIEW

2.1 AIR POLLUTION:

Air pollution, scientifically referred to as atmospheric pollution, encompasses the presence of harmful or excessive concentrations of pollutants in the Earth's atmosphere, leading to adverse effects on human health, ecosystems, and the environment. These pollutants can originate from natural sources such as wildfires, volcanic eruptions, and biogenic emissions, as well as anthropogenic activities including industrial processes, vehicular emissions, agricultural practices, and energy production. Air pollution is characterized by the emission of various pollutants into the atmosphere, including particulate matter (PM), nitrogen oxides (NO_x), sulfur dioxide (SO₂), carbon monoxide (CO), volatile organic compounds (VOCs), ozone (O₃), heavy metals, and air toxics. These pollutants can exist in gaseous form or as suspended particles, with sizes ranging from nanometers to micrometers. The sources of air pollutants vary depending on their chemical composition and emission characteristics (Bonyadi et al., 2021). Combustion processes, such as those occurring in motor vehicles, power plants, and industrial facilities, are major contributors to emissions of NO_x, SO₂, CO, and PM. VOCs are emitted from a wide range of sources, including vehicle exhaust, industrial processes, and solvents. Natural sources such as wildfires, dust storms, and volcanic eruptions can also release significant quantities of particulate matter and gases into the atmosphere (Coudray et al., 2009).

2.2 AIR QUALITY MONITORING:

In contemporary discourse, the adverse impact of substandard air quality on human health and overall well-being stands as a critical concern. Extensive research underscores the association between exposure to air pollutants and a myriad of detrimental health outcomes, notably encompassing respiratory and cardiovascular afflictions, alongside heightened rates of premature mortality. Presently, numerous urban centers and geographical locales across South Asia contend with formidable challenges posed by air pollution. This predicament assumes particular significance within Pakistan, where particulate matter (PM) pollution emerges as a conspicuous issue. Within Pakistani urban

environments, the predominant source of PM emissions stems from residential activities, with heating practices constituting a principal contributor, chiefly reliant on the combustion of fossil fuels and biomass (Li et al., 2020).

Conventional air quality monitoring networks suffer from limited spatial deployment and measurement density due to the high costs associated with the installation and upkeep of monitoring instruments. In the pursuit of advancing high-resolution spatiotemporal monitoring systems for air pollutants, low-cost air quality sensors offer promising adjuncts to regulatory monitors, particularly for assessing exposure to PM_{2.5}. These sensors have demonstrated efficacy in collecting real-time, high-density pollution data and have been developed utilizing Internet of Things (IoT) technologies (Metia et al., 2021). Researchers have also explored augmenting monitoring networks with additional sensors to enhance spatial coverage. Furthermore, low-cost sensors enable real-time acquisition of air quality information across diverse community settings and boast potential advantages in terms of ease of use and maintenance, attributed to their lower energy consumption and spatial requirements (Metia et al., 2021).

Notably, episodes of compromised air quality tend to manifest with greater frequency during the autumn-winter season, with the emission of fine particulate matter, specifically PM_{2.5}, representing a prominent threat to public health and environmental integrity. A proportion of particulate matter (PM) deposits within the respiratory tract traverse deeper into the lower respiratory system, reaching the alveoli, thereby exerting significant adverse effects on health (Lu et al., 2021).

1.2.1 PARTICULATE MATTER:

As described by the United States Environmental Protection Agency (EPA), particulate matter (PM) comprises solid and liquid particles suspended in ambient air, with PM_{2.5} and PM₁₀ representing distinct categories distinguished by their size and inhalation characteristics.

- PM₁₀ denotes particles with a diameter less than 10 micrometers, visible to the naked eye, yet encompassing microscopic constituents.

- PM_{2.5} refers to particles with a diameter less than 2.5 micrometers, primarily microscopic and capable of inhalation by humans.

Both PM₁₀ and PM_{2.5} pose significant health risks, capable of infiltrating the respiratory system and even entering the bloodstream upon inhalation (Bonyadi et al., 2021; Manisalidis et al., 2020; Xing et al., 2016).

Particulate matter is further classified into primary and secondary groups, delineating direct emissions versus particles formed through atmospheric transformations. Primary particles originate directly from emissions sources, whereas secondary particles arise from the oxidation or chemical transformation of precursor compounds in the atmosphere. These precursor compounds include volatile organic compounds (VOCs), sulfur oxides (SO_x), and nitrogen oxides (NO_x). Interactions among these gaseous constituents lead to the formation of secondary particles, often through the condensation of acids produced during chemical reactions (Orach et al., 2021). These acids facilitate the aggregation of small droplets by absorbing water vapor from the ambient atmosphere. The origins of PM₁₀ are diverse and encompass a range of sources, including fly ash, dust, coal combustion residues, metal oxides derived from crustal components, and mechanical abrasion of surface materials (Sahu et al., 2020). Additionally, PM₁₀ can result from physical processes such as wind erosion and vehicular traffic. These varied sources contribute to the complex composition and dynamics of particulate matter in the atmosphere, underscoring the multifaceted nature of air pollution and its implications for human health and environmental quality.

2.3 LOW-COST AIR QUALITY MONITORING SENSORS AND NETWORKS:

Ensuring the precision of monitoring and predictive systems for real-time assessment of air quality emerges as a paramount concern in urban locales. Particularly noteworthy is the recent proliferation of Internet of Things (IoT) technologies (Metia et al., 2021), which has facilitated the rapid development of low-cost wireless sensor networks (LWSN) serving as localized monitoring infrastructures. These systems are integrated with conventional already installed observatories to augment the spatiotemporal resolution of environmental parameters. However, given the continuous exposure of these sensors to fluctuations in

weather patterns during their round-the-clock operation, the imperative to devise robust and dependable monitoring systems is evident to enhance performance reliability.

Low-cost air quality monitoring sensors (Bilgiç et al., 2021; Metia et al., 2021) represent a burgeoning field within environmental monitoring, enabled by advancements in technology, particularly the Internet of Things (IoT). These sensors are designed to provide real-time data on various air pollutants, including particulate matter (PM_{2.5}), volatile organic compounds (VOCs), nitrogen dioxide (NO₂), and ozone (O₃), among others (Lin et al., 2017). Typically, these sensors utilize compact and low-power designs, allowing for easy deployment in diverse urban environments. They leverage a range of sensing techniques, such as optical, electrochemical, and metal oxide semiconductor technologies, to detect and quantify pollutant concentrations. Additionally, low-cost sensors often incorporate wireless connectivity, enabling seamless data transmission to centralized monitoring platforms. The deployment of low-cost air quality monitoring sensors is integral to the establishment of dense sensor networks, which aim to enhance spatial coverage and resolution of air quality monitoring in metropolitan areas. These sensor networks are strategically positioned across urban landscapes, including streets, parks, and residential areas, to capture localized variations in pollutant concentrations. By leveraging IoT infrastructure, these sensors communicate with each other and with centralized data servers, facilitating real-time monitoring and analysis of air quality parameters. Moreover, the data collected from these sensors can be integrated with existing air quality monitoring networks operated by government agencies or research institutions, augmenting their capabilities for pollutant assessment and forecasting. Despite their affordability and scalability, low-cost air quality monitoring sensors present certain challenges related to data accuracy and reliability (Badura et al., 2019). Factors such as sensor drift, cross-sensitivity to environmental conditions, and calibration issues may impact the accuracy of pollutant measurements. Thus, ongoing research efforts focus on improving sensor performance through advanced calibration techniques, data fusion algorithms, and quality assurance measures. Additionally, the development of open-access data standards and quality control protocols is critical to ensuring the integrity and interoperability of data collected from diverse sensor networks. In conclusion, low-cost air quality monitoring sensors and networks hold significant promise for revolutionizing urban air quality

management, offering cost-effective solutions for enhancing public health and environmental sustainability.

2.4 WILDFIRES AND BUSHFIRES:

Wildfires and bushfires are natural phenomena characterized by uncontrolled and extensive burning of vegetation in forested and grassland areas, respectively (Bilgiç et al., 2021). These events result from the ignition and rapid spread of flames across vast expanses of flammable biomass, driven primarily by environmental factors such as dry conditions, high temperatures, and strong winds. Wildfires typically occur in forested regions, encompassing densely wooded areas with ample fuel sources, including trees, shrubs, and ground vegetation. Conversely, bushfires predominantly affect grassland ecosystems, where combustible vegetation such as grasses, shrubs, and scrublands serve as the primary fuel for fire propagation (Hosseini et al., 2010). The ignition of wildfires and bushfires can arise from various sources, including lightning strikes, human activities such as campfires, agricultural burning, and accidental ignition from power lines or machinery. Once ignited, these fires can exhibit rapid and erratic behavior, spreading rapidly and unpredictably across the landscape, driven by the interplay of weather conditions, topography, and fuel availability. The intensity and severity of wildfires and bushfires can vary widely, ranging from small, localized burns to large-scale conflagrations that engulf thousands of hectares of land and pose significant threats to ecosystems, human settlements, and infrastructure. In addition to their immediate impacts on vegetation and landscape dynamics, wildfires and bushfires can have far-reaching environmental, social, and economic consequences. They contribute to air pollution through the release of smoke, particulate matter, and harmful gases, exacerbating respiratory ailments and compromising air quality over extensive geographic areas (Hosseini et al., 2010). Furthermore, these events can lead to habitat destruction, loss of biodiversity, soil erosion, and altered hydrological regimes, with long-term implications for ecosystem functioning and resilience.

In human-populated areas, wildfires and bushfires pose significant risks to public safety and property, necessitating evacuation measures, firefighting efforts, and emergency response operations. The threat of wildfire occurrence and its potential impacts on

communities underscore the importance of proactive fire management strategies, including fire prevention, preparedness, and mitigation measures (Jiang & Bell, 2008; Prado et al., 2012). Through effective land management practices, prescribed burning, fire suppression techniques, and community engagement initiatives, stakeholders can work to reduce the incidence and severity of wildfires and mitigate their adverse effects on ecosystems, livelihoods, and well-being.

2.4.1 FORESTS:

Forests represent complex ecosystems characterized by the predominant presence of trees, encompassing diverse biotic and abiotic components within a defined geographic area. Scientifically, forests are classified based on various criteria such as tree species composition, structure, climate, and ecological functions (Bilgiç et al., 2021). They play pivotal roles in global carbon cycling, biodiversity conservation, water regulation, and provision of ecosystem services. From a botanical perspective, forests are distinguished by their canopy layer, comprising the uppermost layer of tree crowns that collectively form a dense covering over the forest floor. Beneath the canopy, multiple vertical layers including the understory, shrub layer, and herbaceous layer contribute to the structural and functional diversity of forest ecosystems. Tree species within forests exhibit varying growth forms, life histories, and ecological niches, influencing forest structure, dynamics, and species interactions.

2.4.2 TEMPERATE FORESTS:

Temperate forests are characterized by moderate temperatures and ample rainfall, typically occurring in regions with distinct seasons. These forests are predominantly composed of broadleaf deciduous trees such as oak, maple, beech, and birch in the Northern Hemisphere, while species like eucalyptus and southern beech may dominate in the Southern Hemisphere. They undergo seasonal changes, with trees shedding leaves in autumn and regenerating foliage in spring (Norovsuren et al., 2019). These forests support a rich diversity of plant and animal life, including mammals, birds, reptiles, and amphibians. Examples of temperate forests include those found in North America, Europe, and parts of Asia.

2.4.3 *MIXED FORESTS:*

Mixed forests feature a combination of coniferous and broadleaf trees and are often located in transitional zones between pure coniferous and deciduous forests. Tree species such as pine, spruce, fir, oak, beech, and maple may coexist, depending on local environmental conditions. Mixed forests exhibit intermediate characteristics between purely coniferous and deciduous forests, with varying degrees of tree species diversity and ecological processes. They occur in regions with diverse climates, including temperate, subarctic, and montane environments. Examples of mixed forests can be observed in regions such as the Pacific Northwest of North America, parts of Europe, and the Himalayan region.

2.4.4 *MEDITERRANEAN FORESTS:*

Mediterranean forests thrive in regions characterized by a Mediterranean climate, typified by hot, dry summers and mild, wet winters. These forests are dominated by evergreen sclerophyllous trees adapted to drought conditions, such as oaks, pines, cypresses, and olive trees. Due to the climatic conditions, vegetation in Mediterranean forests tends to be adapted to withstand prolonged periods of drought. These forests are notable for their ecological resilience and support a variety of flora and fauna uniquely adapted to the Mediterranean climate. Examples of Mediterranean forests can be found in regions bordering the Mediterranean Sea, including parts of Southern Europe, North Africa, and the Middle East.

2.4.5 *GRASSLANDS (STEPPE):*

Grasslands, scientifically referred to as "prairies," "steppes," or "savannas," are ecosystems characterized by vast expanses of grasses, herbs, and non-woody vegetation, with relatively few trees or shrubs. They are typically found in regions with semi-arid to sub-humid climates, where precipitation is sufficient to support vegetation growth but insufficient to sustain extensive forests. Grasslands occur on every continent except Antarctica and play crucial ecological roles in the global carbon cycle, biodiversity conservation, and ecosystem services provisioning. Grasslands are also characterized by their resilience to disturbance, particularly fire and grazing. Fire, whether natural or anthropogenic, plays a

vital role in maintaining grassland ecosystems by suppressing woody vegetation, promoting nutrient cycling, and stimulating seed germination. Grazing by herbivores, including ungulates such as bison, antelope, and zebras, contributes to the dynamic balance of grassland ecosystems by regulating vegetation structure and composition.

2.4.6 SCRUBLANDS:

Scrublands, also known as shrublands or chaparral, represent ecosystems characterized by low-growing woody vegetation, primarily consisting of shrubs, bushes, and small trees, interspersed with grasses and herbaceous plants. These ecosystems typically occur in regions with semi-arid to Mediterranean climates, characterized by hot, dry summers and mild, wet winters. scrublands are classified as a distinct vegetation type characterized by the prevalence of shrubby vegetation adapted to thrive in nutrient-poor soils and water-stressed environments. The dominant plant species in scrublands often exhibit adaptations such as deep root systems, drought-resistant foliage, and fire-tolerant traits, enabling them to survive and persist in harsh ecological conditions.

Scrublands play important ecological roles in nutrient cycling, soil stabilization, erosion control, and habitat provision for a variety of wildlife species. They support diverse flora and fauna adapted to the unique environmental conditions of scrubland ecosystems, including birds, reptiles, small mammals, and insects. Many species found in scrublands have evolved specialized adaptations to survive in these harsh habitats, such as nocturnal behavior, heat tolerance, and water conservation strategies.

2.5 ABOVE-GROUND BIOMASS:

Aboveground biomass refers to the total mass of living plant material present above the ground surface within a defined area of an ecosystem. This biomass comprises the collective weight of all components of vegetation that are visible above the soil, including stems, branches, leaves, flowers, fruits, and reproductive structures. Aboveground biomass plays a fundamental role in ecosystem structure, functioning, and carbon cycling processes, serving as a primary indicator of vegetation productivity, biomass allocation patterns, and carbon sequestration potential. The composition and distribution of aboveground biomass

vary across different vegetation types and ecosystems, influenced by factors such as climate, soil fertility, disturbance regimes, and plant species composition. In dense forests, aboveground biomass is predominantly composed of tall trees with extensive canopies, large branches, and abundant foliage, contributing significantly to the overall biomass accumulation. In contrast, in open grasslands and shrublands, aboveground biomass is characterized by low-growing vegetation, including grasses, shrubs, and herbs, with relatively lower biomass densities compared to forests.

Quantifying aboveground biomass is crucial for understanding ecosystem dynamics, assessing carbon stocks, and monitoring changes in vegetation structure and productivity over time. Various methods, including field measurements, remote sensing techniques, and allometric equations, are employed to estimate aboveground biomass at different spatial scales, ranging from individual plants to entire landscapes. These methods utilize parameters such as tree diameter, height, canopy cover, and vegetation indices derived from satellite imagery to derive accurate estimates of biomass density and carbon content. Aboveground biomass serves as a vital reservoir of carbon in terrestrial ecosystems, playing a critical role in mitigating atmospheric carbon dioxide concentrations through photosynthesis and carbon sequestration. As such, changes in aboveground biomass stocks have significant implications for global carbon cycling, climate change mitigation efforts, and biodiversity conservation initiatives. Monitoring and managing aboveground biomass resources are essential for maintaining ecosystem health, resilience, and sustainability in the face of environmental change and anthropogenic pressures.

CHAPTER 3: METHODOLOGY

3.1 DETAILED OUTLINE OF METHODOLOGY:

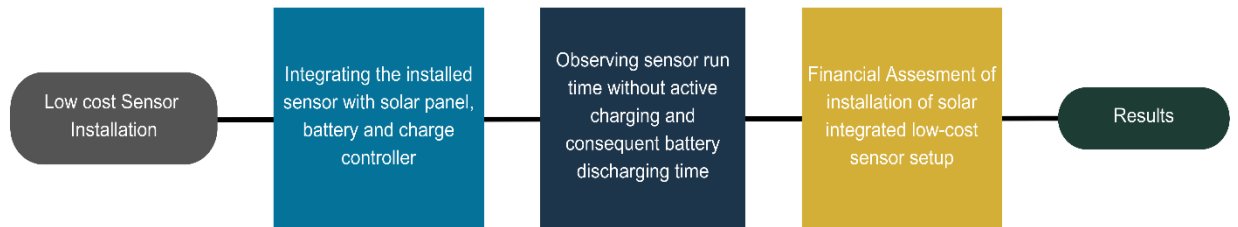


Figure 1.1 Process flow diagram for methodology against Objective 1

The flowchart outlines the methodology for assessing the technical and financial feasibility of transforming a low-cost sensor to operate on solar power, corresponding to the first objective of your thesis. The process starts with the installation of a low-cost sensor. Once installed, the sensor is integrated with a solar panel, a battery, and a charge controller. This integration is crucial for harnessing solar energy to power the sensor and involves ensuring that the components work harmoniously. Following the integration, the next step involves observing the sensor's performance, specifically its runtime without active charging and the subsequent battery discharging time. This observation helps in understanding how long the sensor can operate solely on battery power, which is critical for assessing the reliability and efficiency of the solar-powered setup.

The subsequent step is the financial assessment of the solar-integrated low-cost sensor setup. This involves evaluating the costs associated with the installation and maintenance of the solar panel, battery, and charge controller, compared to the benefits of using solar power over traditional power sources. Factors such as initial investment, potential savings on energy costs, and long-term financial benefits are considered in this assessment. Finally, the results of these assessments are compiled. The results provide a comprehensive understanding of both the technical feasibility and the financial viability of converting low-cost sensors to solar power.

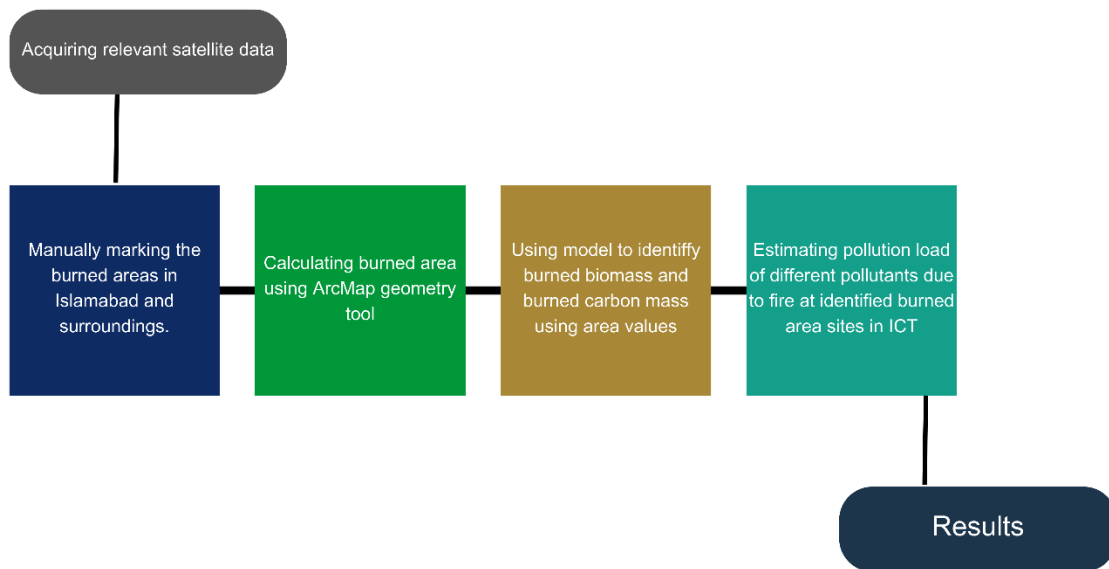


Figure 3.2 Process flow diagram for methodology against Objective2

The flowchart illustrates the methodology for assessing the emissions of pollutants during wildfire activity around Islamabad Capital Territory (ICT) in May-June 2022, utilizing a Biomass Combustion Model. The process begins with acquiring relevant satellite data, which serves as the foundational data source for the analysis. The first step involves manually marking the burned areas in Islamabad and its surroundings using the satellite data. This manual marking ensures accuracy in identifying the specific areas affected by wildfires. Once the burned areas are marked, the next step is calculating the burned area using the ArcMap geometry tool. This tool allows for precise measurement of the area affected by the wildfires, providing essential data for further calculations.

Following the calculation of the burned area, a model is employed to identify the burned biomass and the burned carbon mass using the area values obtained. This step is crucial for understanding the amount of biomass consumed by the fire and the corresponding carbon

emissions. The subsequent step involves estimating the pollution load of different pollutants released due to the fire at the identified burned area sites in ICT. This estimation includes various pollutants that are typically emitted during wildfires, such as particulate matter, carbon monoxide, and other harmful gases. Finally, the results of these assessments are compiled. The results provide a comprehensive understanding of the emissions of pollutants during the wildfire activity around ICT.

3.2 TSI LOW-COST AM SENSORS:

For the purpose of monitoring ambient air quality in Islamabad and Rawalpindi, TSI low-cost air quality monitoring sensors were used. The TSI BlueSky™ Air Quality Monitor is a lightweight, laser-based particle instrument designed to simultaneously measure PM_{2.5} and PM₁₀ mass concentrations, as well as temperature and relative humidity. As an Internet of Things (IoT) solution, these hyperlocal, cloud-based air quality monitors offer data interfacing using WiFi, and comes standard with an SD memory card for duplicate data storage, software and cloud data services (Metia et al., 2021). While specifically designed for outdoor environmental monitoring, BlueSky Air Quality Monitors can also be utilized inside buildings, homes and manufacturing facilities to measure indoor air quality.



Figure 3. 3 Top view (left) and bottom view (right) of TSI BlueSky Low-cost Air Quality Monitoring Sensor

Before deployment, each individual sensor unit needs to be registered at TSI cloud with its individual serial number and password with user's account on the cloud. Once registered, the sensor unit needs to be deployed at desired location, with easy flow of air. As soon as the sensor is connected to an active Wifi (internet) source, it starts uploading real-time data on the cloud site. The minimum resolution of data recording is 1 minute interval. The dataset can either be downloaded in MS Excel sheet directly via the cloud or by detaching the SD card placed inside the sensor.

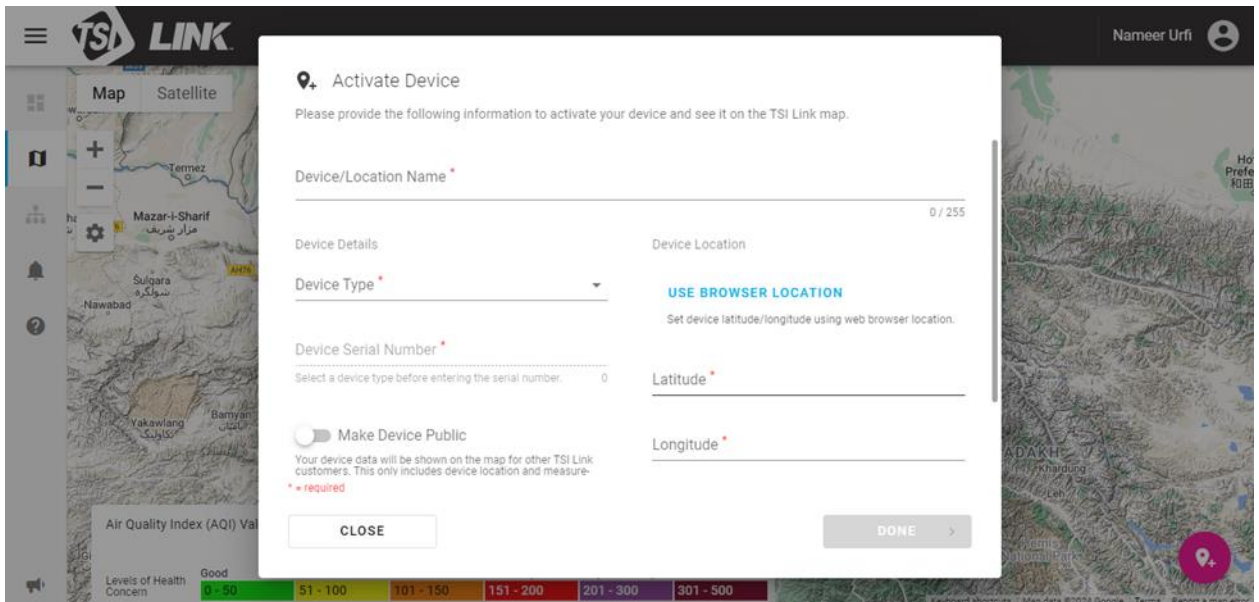


Figure 3. 4 User interface of TSI cloud site for registering the devices online before installment. Location and type of devices are added manually.

The data provided is of PM_{2.5}, PM₁₀ in ug/m³ while of temperature in centigrade while of relative humidity in percentage.

3.2.1 PURPOSE OF USING TSI LOW-COST SENSORS:

The purpose of using specifically TSI BlueSky low-cost sensors was purely the easy availability of these sensors. These specific sensors were used as part of a Duke University, US Department of State project titled, “Building Capacity to Improve Air Quality in South Asia: Reducing PM_{2.5} Through Low-Cost Sensor Network Driven Policy Decisions”. Under this project, more than 50 low-cost sensors were installed across major cities of

Pakistan to develop a seasonal air quality profile of these cities in comparison to already installed conventional air quality monitoring technologies at annual basis.

3.2.2. LIMITATIONS OF LOW-COST SENSORS:

Although low-cost air quality monitoring sensors are easy to use and deploy as compared to conventional technologies as mentioned above, yet there are some limitations that need to be addressed while using these sensors which are given as follows:

- Low-cost air quality monitoring sensors require active power supply to run. They do not come with integrated battery or a solution to run them without a power source even for a few hours which makes their deployment in a remote area quite challenging.
- Similarly, low-cost sensors need an all-time active internet wifi connection to stay connected to cloud and provide the real-time data, yet they do not come with a built in connecting mechanism. If to be deployed remotely, they need to be provided with an external internet source.

3.3 INTEGRATION WITH SOLAR PANEL:

In order to overcome the limitations mentioned above, the low-cost sensors needed to be integrated with an off-grid independent power source to keep it running. To solve this issue, the individual sensor unit was made to get connected with a solar panel and a battery to store charge in case of any backup scenario. The solar panel, battery and sensor assembly was arranged as shown in the figure below:

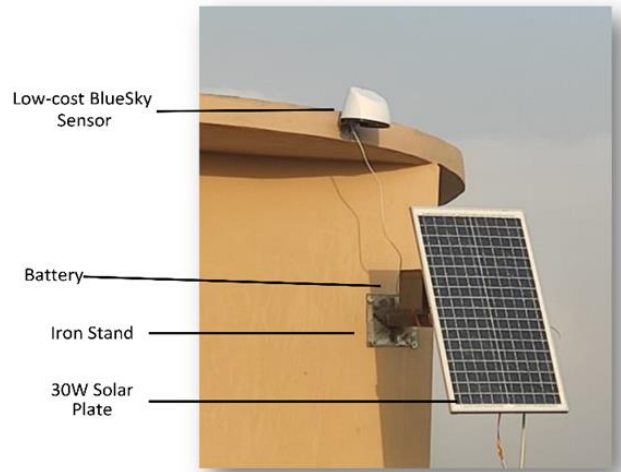


Figure 3. 5 Solar integrated assembly of low-cost air quality monitoring sensor at IESE, NUST

3.3.1. SOLAR PANEL SPECIFICATIONS:

The solar panel used to develop solar integrated low-cost sensor was selected based on the requirement of being able to power enough backup to sensor to run with minimum amount of sunlight for about 2 days. The specifications of the solar panel are as follows:

Table 3.2 Solar panel specifications for wireless independent low-cost air quality sensor

Solar Plate	30W
Maximum Power	30W
Maximum Voltage	18V
Max. Power Current	1.56A

For assessing the feasibility of solar integrated low-cost sensor, two scenarios were observed in real-time to monitor the effectiveness of selected specification equipment which are as follows:

Scenario 1:

The first scenario was to assess the time taken by battery to completely charge by 30W solar plate simultaneously powering a 3W air quality sensor and 2W internet dongle device.

The assembly was placed at the roof of IESE, NUST to observe the timings and following observations were made:

Table 3.3 Conditions for first scenario for observing technical feasibility of solar power backup with low-cost sensor

Plug-in Date	15/11/2022
Plug-in Time	0930 hrs
Charged Date	18/11/2022
Charged Time	1215 hrs
Total Charge Time	74 hrs

Validation:

To validate this observation, following calculations were theoretically done:

Box 1 Theoretical calculation for battery charge time while connected to sensor

<p>Current (I) = Power (W) / Voltage (V) = 30W / 18V = 1.67A Energy per day = Current × Time = 1.67A × 8 hours = 13.36Ah/day Actual energy per day = 13.36Ah/day × 0.85 = 11.35Ah/day (Assuming 85% efficiency of solar panel) Total consumption per day: Battery = 26Ah/day Devices: [(3.5W+2W) x 24hrs] / 12V = 11Ah Consumption/day = 26+11 = 37Ah/day Time to charge battery = 37/11.35 = 3.2 days = 76 hrs (approx.)</p>

Scenario 2:

The second scenario was designed to assess the battery discharge time while unplugged from the solar plate and powering both the devices i.e internet dongle and low-cost sensor.

In the similar assembly placed at the roof of IESE, NUST following observations regarding battery discharge were made:

Table 3.4 Conditions for second scenario for observing technical feasibility of solar power backup with low-cost sensor

Start Date	21/11/2022
Start Time	1030 hrs
Stop Date	25/11/2022
Stop Time	0850 hrs
Total Discharge Time	94 hrs (approx.)

To validate the observations, following calculations were theoretically done:

Box 2 Box 1 Theoretical calculation for battery discharge time while connected to sensor

<p>Time (discharge) = Battery Capacity / Device Power</p> <p>convert the battery capacity from ampere-hours (Ah) to watt-hours (Wh) since both the battery capacity and device power need to be in the same units for the calculation</p> <p>Battery Capacity (Wh) = Battery Capacity (Ah) x Voltage = 26Ah x 12V = 312Wh Now, synching both the units,</p> <p>Time (discharge) = Battery Capacity / Device Power = 312Wh / 3.5W = 89.15 hrs</p> <p><i>Note: Disparity of about 4 hours in observed and calculated time might be due to observational error, or disconnection of sensor during operation</i></p>
--

3.4 FINANCIAL FEASIBILITY:

After assessing the technical feasibility of integrating low-cost air quality monitoring sensor with the solar panel and a backup battery, financial feasibility of the assembly was also done. The main purpose of designing this assembly was to eliminate the limitation of these sensors of not being able to receive power and internet in remote areas. This assembly

would allow the deployed sensor to have uninterrupted power supply along with wireless internet.

The financial feasibility of installing 30 such assemblies including the labor cost for installation will be as follows:

Table 3.5 Financial feasibility of integrating low-cost sensor with solar power backup

Item	Solar Plate	Battery	Charge Controller
Size	30W	312Wh (12V-26Ah)	3amp
Price	5000.00	12,000.00	1,000.00
Price for 30	150,000.00	360,000.00	30,000.00
Total Cost per Unit	18,000.00		
Total Cost per 30 Units	540,000.00		

Adding a labor cost of Pkr1000 per each installation, the total cost of installation will rise up to be Rs 570,000/-.

3.5 FIRE EVENT INITIAL ASSESSMENT:

In this study, we have examined the pollutants released during intense bushfire episodes occurred in NUST Islamabad on June 7th to 8th, 2022. These episodes resulted in the accumulation of a significant amount of dry litter and vegetation fuel, causing a burnt area of 0.6567 km². As a consequence, a substantial amount of pollutants were introduced into the environment of NUST. To assess the impact of these bushfires on local air quality, we employed in-situ observations using low-cost sensors and satellite observations and quantified their contribution to the enhancement of PM concentrations over NUST. There were 5 VIIRS fire alerts reported between 7th to 8th June 2022 on Sentinel 2A, 10m x 10m satellite imagery. The TSI devices NUSTpk-3 and NUSTpk-6 deployed at IESE NUST, indicated a clear enhancement in PM_{2.5} concentrations during bush fire event. Furthermore, the wind direction during this period was from the South and Southeastward, which likely influenced the readings of the low-cost sensors that were deployed in the same direction as

the air flow. These findings provide scientific evidence of the impact of the bushfires on local air quality, as observed through satellite data and on-site sensor measurements.

4 STUDY AREA:

National University of Science and Technology (NUST) is located near Kashmir Highway H-12, Islamabad. The campus is spread over 2.86 km² of land. In the present study, measurements of PM are made at Institute of Environmental Sciences and Engineering (IESE) 41.3936° N, 2.1057° E. The climate of Federal Capital Islamabad is humid subtropical where winters are very cold while summers are moderately hot. During summer, the average temperature is around 25–35°C and can rise up to 40°C.

5 DATA SETS:

The data was acquired from the VIIRS developed products by APPEARS, NASA, which provided information on the active burning sites on 8th June, 2022 around Islamabad and Rawalpindi. The study focuses on the Islamabad Capital Territory (ICT) and the Margalla Hills, where the active fire events were observed during the day. In particular, the study investigates the NUST campus, which is located in the region, and the occurrence of active fire spots in the hiking trail area. The reasons for the active fires in the bushes of the NUST campus may be attributed to various factors. Firstly, the campus was built on a previously existing dumping site, which could have resulted in the leakage of methane packets from under the soil. Secondly, the extreme temperatures in the area could have triggered the dry biomass, which spread across the campus area. To estimate the above ground biomass and burned areas of the campus, the study used a number of satellite products from Sentinel-1A and Sentinel-2A.

The ground-based data information was taken from ground-based monitoring stations. PM_{2.5} validation was done using the low-cost air quality monitors developed by TSI-BlueSky. These monitors provide real-time PM_{2.5} data with a resolution of 1 minute. These monitors were located at the roof of IESE, NUST along with other air quality monitoring instruments and weather station.

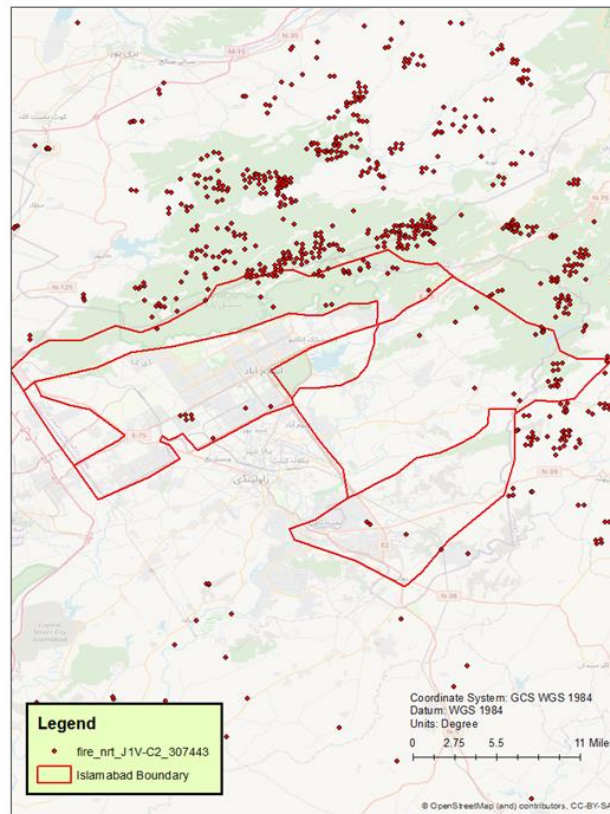


Figure 3. 6 Active fire points of Islamabad Capital Territory and surroundings on 8th June, 2022

6 BURN AREA DETECTION:

The frequency and extent of fires in Pakistan is very variable from year to year, reflecting year-to-year climatological variability. Emissions from forest fires depend on following

1. the duration and intensity of the fire
2. the total area burnt by the fire, and
3. the type and amount of vegetation that is burnt.

This latter term is often referred to as fuel load. Of those three terms, the one that is known with a fair level of accuracy is the total burnt area. In order to conduct an analysis of the burned area in the NUST Campus, a manual detection method was employed. Specifically, composite images from Sentinel-2A with a high resolution of 10m x 10m were analyzed using ArcMap 10.8. To facilitate the analysis, polygons were manually drawn over the area

that was burned within the region of interest, which in this case was the Islamabad Capital Territory area.

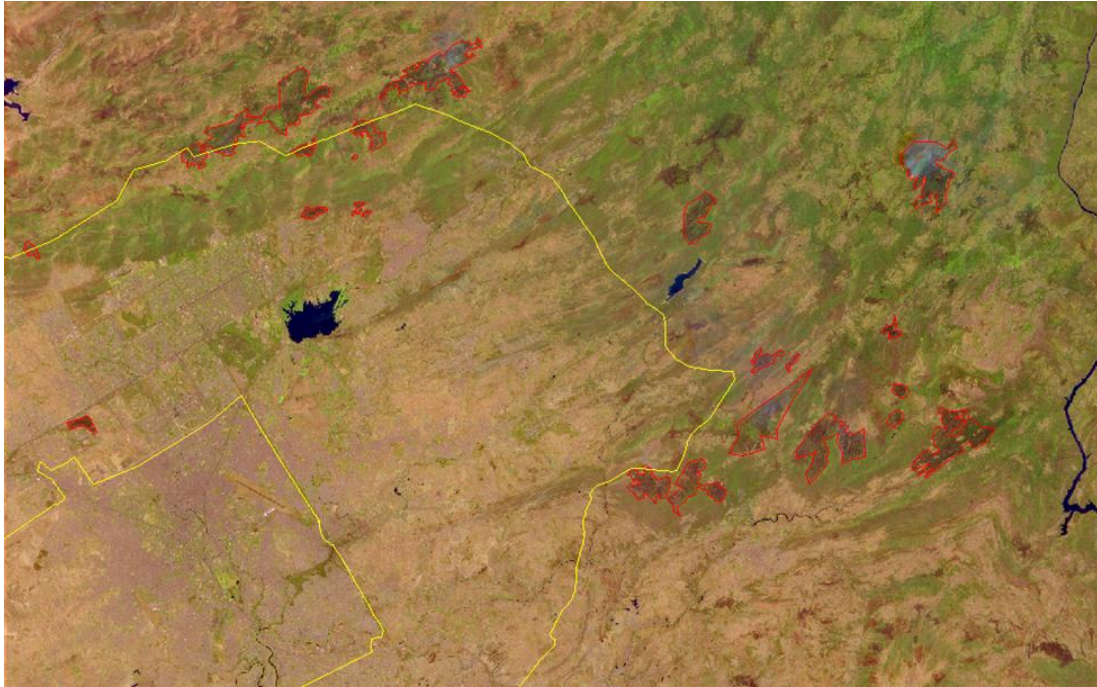


Figure 3. 1 Sentinel 2-A 20m x 20m resolution RGB image of active fires and burned areas in and around Islamabad Capital Territory manually marked using ArcMap 10.8

PRE-FIRE/POST-FIRE VISUALIZATION:

The fire locations can also be confirmed by doing a visual analysis of Sentinel 2A RGB image analysis of pre-fire dates i.e June 6, 2022 and a post-fire date i.e. June 8, 2022. This image visualization confirms active fire events at multiple locations within and around Islamabad Capital Territory specially at NUST site.

In the images, the difference in the burnt area can clearly be seen as the burnt areas are darker shaded as compared to unburnt vegetation.

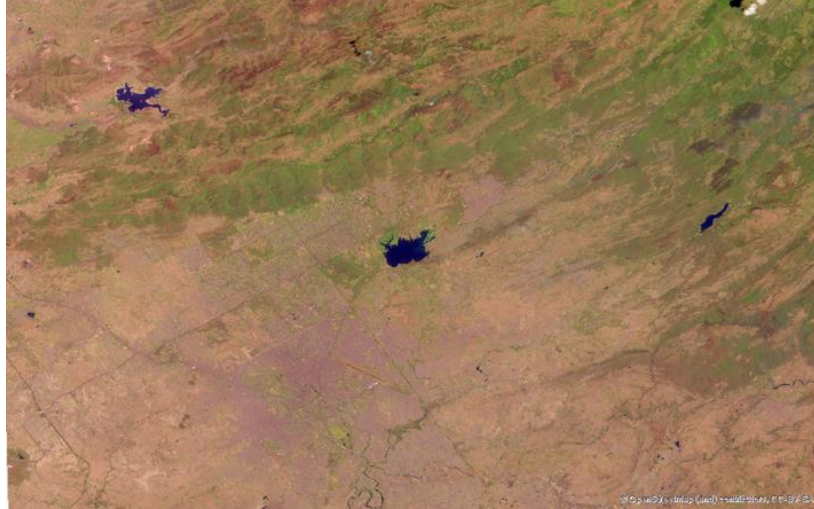


Figure 3. 7 Sentinel 2-A 20m x 20m resolution RGB image of active fires and burned areas in and around Islamabad Capital Territory on 6th June, 2022



Figure 3. 8 Sentinel 2-A 20m x 20m resolution RGB image of active fires and burned areas in and around Islamabad Capital Territory on 8th June, 2022

7 SYNTHETIC APERTURE RADAR (SAR) VISUALIZATION:

Synthetic Aperture Radar (SAR) data is a type of remote sensing data collected by radar sensors mounted on satellites or aircraft. SAR systems emit microwave signals towards the Earth's surface and record the signals reflected back. By measuring the time delay and phase shifts of these reflected signals, SAR systems generate high-resolution images of the Earth's surface. The purpose of visualizing SAR data to validate the burnt area is because of the following characteristic advantages:

- It can penetrate through clouds, haze, and darkness, allowing for imaging in all weather conditions and during day or night.
- It provides information about surface roughness, terrain elevation, and moisture content, which may not be readily available from optical sensors.
- SAR systems can also detect small movements on the Earth's surface, making them useful for monitoring changes such as ground subsidence or deformation.

3.9.1 DATA PRODUCTS OF SAR:

SAR data is typically processed to generate various products, including:

- Single Look Complex (SLC) images: These are complex-valued images that retain the phase information of the radar signal.
- Ground Range Detected (GRD) images: These are amplitude images that have undergone processing to remove geometric distortions.
- Interferometric SAR (InSAR) products: By comparing phase differences between SAR images acquired from slightly different angles, InSAR can generate maps of surface elevation or detect ground deformation.

In this study, GRD images of SAR were processed for visualization.

Sentinel 1-A:

Sentinel-1A is a satellite mission launched by the European Space Agency (ESA) as part of the Copernicus program. It carries a Synthetic Aperture Radar (SAR) sensor operating in the C-band frequency range. The SAR sensor on Sentinel-1A offers several polarization modes, including:

- Single Polarization (HH or VV): Transmitting and receiving signals in either horizontal (HH) or vertical (VV) polarization.
- Dual Polarization (HH+HV or VV+VH): Simultaneous transmission and reception of signals in two different polarizations, such as horizontal-horizontal (HH+HV) or vertical-vertical (VV+VH).

Sentinel-1A SAR data typically provides spatial resolutions ranging from a few meters to tens of meters, depending on the imaging mode and processing level. The Ground Range Detected (GRD) products, for instance, offer spatial resolutions of about 20 meters. It has a high revisit frequency, with the satellite acquiring data over the same area every few days. This frequent revisiting enables monitoring of dynamic phenomena such as crop growth, urban expansion, and natural disasters. It covers a wide swath width, typically up to 250 kilometers, allowing for large-scale mapping and monitoring applications.

Application:

Sentinel-1A SAR data is used for a wide range of applications, including:

- Land cover and land use classification.
- Agriculture monitoring, including crop type mapping and yield estimation.
- Forest monitoring, including deforestation detection and biomass estimation.
- Urban planning and monitoring, such as infrastructure development and land subsidence detection.
- Disaster management, including flood mapping, earthquake damage assessment, and monitoring of volcanic activity.

3.9.2 SAR DATA FOR THIS STUDY:

The study employed Sentinel-1A Synthetic Aperture Radar (SAR) C-band data in interferometric wide swath mode. This mode featured a swath width of 250 kilometers and achieved a spatial resolution of 5 by 20 meters. The incidence angle ranged from 29.1 degrees to 46.0 degrees, facilitating comprehensive coverage of the target area. Dual polarizations, VV (vertical-vertical) and VH (vertical-horizontal), were utilized to enhance the versatility of the dataset (Al-Hasn & Almuhammad, 2022).

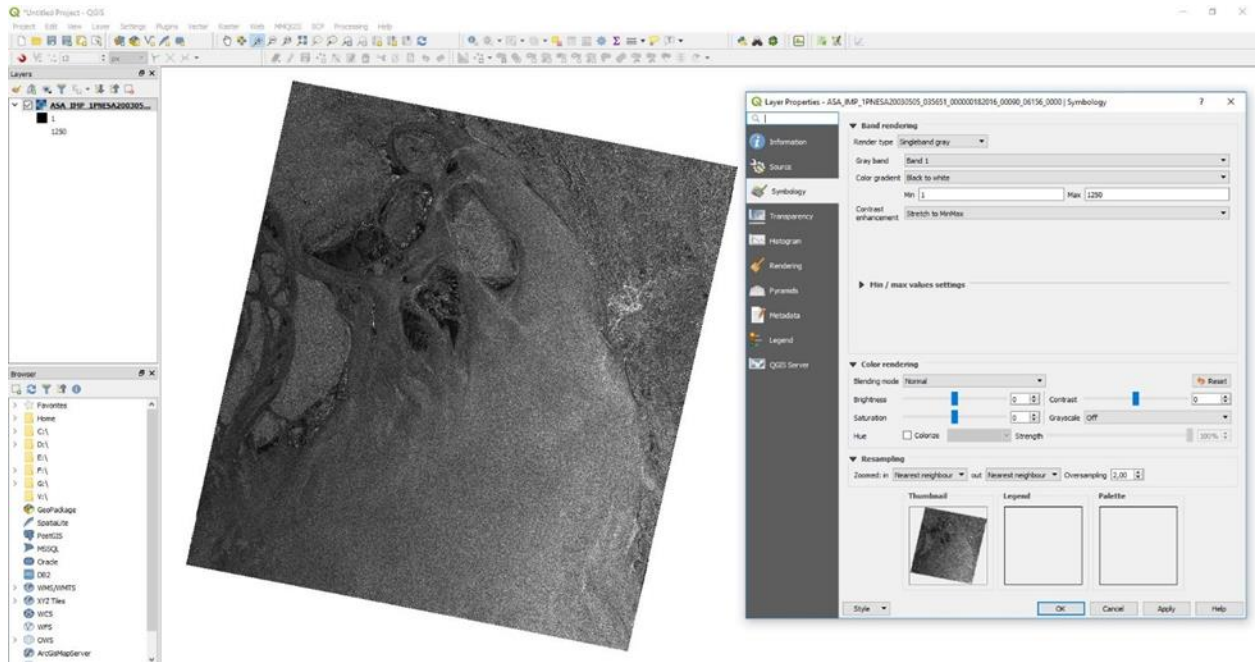


Figure 3.9 User interface of SNAP (Sentinel Application Platform) version 4.0.0 while processing a C-Band image from Sentinel 1-C

Data processing was conducted utilizing the Sentinel Application Platform (SNAP) version 4.0.0, a software suite developed by the European Space Agency (ESA). The processing workflow included several key steps to derive useful information from the SAR data. Firstly, radiometric calibration was performed to obtain sigma 0 values, ensuring consistency and accuracy in the radar backscatter measurements. Subsequently, speckle filtering techniques were applied to reduce noise and enhance the clarity of the SAR images. Calibration procedures were then implemented to correct for system-induced distortions and variations in sensor response. Furthermore, range-Doppler terrain correction was conducted utilizing the Shuttle Radar Topography Mission (SRTM) digital elevation model. This correction accounted for variations in terrain elevation, thereby improving the accuracy of geometrically corrected SAR imagery. Finally, the backscatter values were converted from linear to decibel scale, enabling easier interpretation and analysis of the radar signal intensities.

3.9.3 SAR Visualized Burned Area:

Using SAR data visualization, following image was generated clearly pointing out the burned area in NUST H-12 Campus trail as shown in the following image:

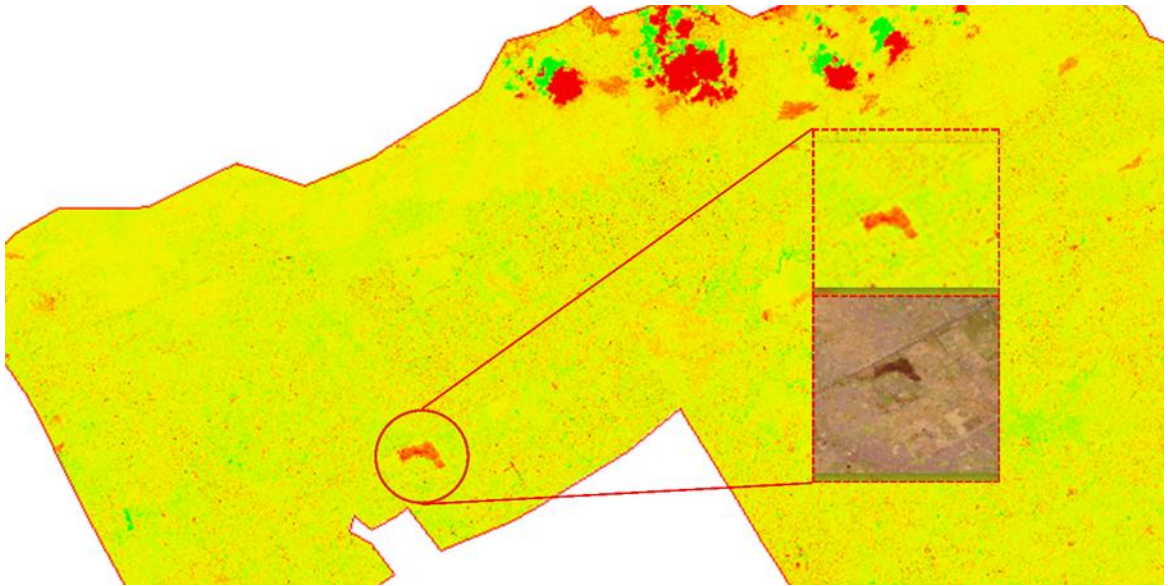


Figure 3. 10 Burned area at NUST H-12 Campus visualized in VV-VH C-band calibrated and corrected image of Sentinel 1-C

3.10 NORMALIZED BURN RATIO:

The Normalized Burn Ratio (NBR) is an index that is specifically designed to feature burnt areas in large fire regions. This index is calculated using the near-infrared (NIR) and shortwave infrared (SWIR) wavelengths according to a specific formula. In the present study, we utilized this formula to determine the NBR values (Al-Hasn & Almuhammad, 2022) for the burnt areas in the NUST Campus.

As part of the analysis, the second step involved calculating the Normalized Burn Ratio (NBR) and assessing the Delta Normalized Burn Ratio (dNBR) values. This was achieved by analyzing satellite images using the ArcMapv10.8 platform. Moreover, we assessed the Delta Normalized Burn Ratio (dNBR) values, which are used to quantify the severity of the burn area. These values were calculated by subtracting the pre-fire NBR values from the post-fire NBR values. The result is a measurement of the change in vegetation and biomass cover that has occurred due to the fire. NBR can be estimated using the following equation:

$$NBR = \frac{NIR - SWIR}{NIR + SWIR}$$

$$dNBR = NBR_{post} - NBR_{pre}$$

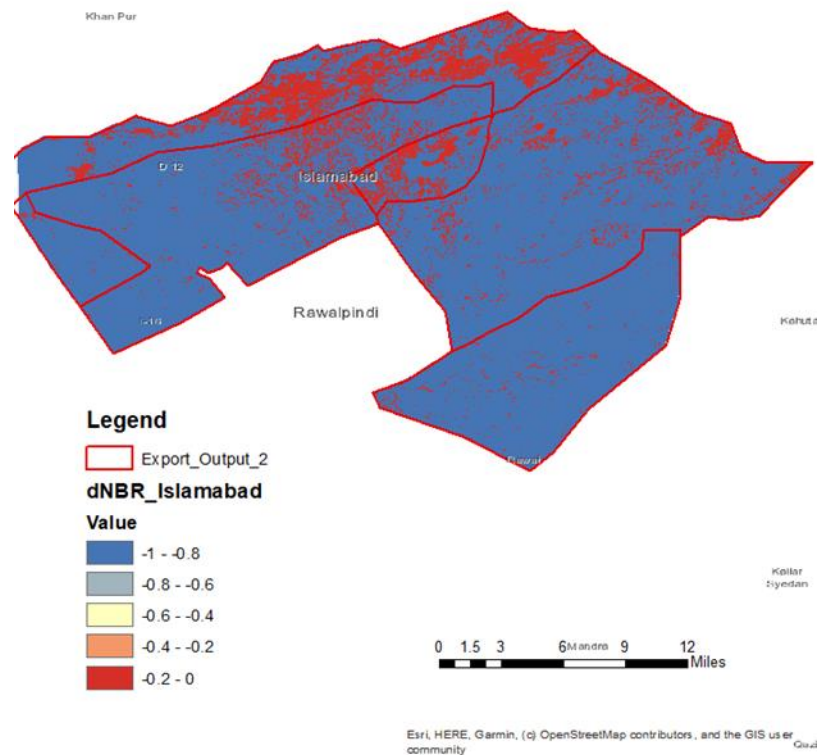


Figure 3. 11 Delta-NBR index for fire in ICT classified maximum (highest severity) to minimum (lowest severity)

3.11 EMISSION ESTIMATION:

After the estimation of burn ratio and identification of burn areas, the next step in this study was estimation of emissions due to the fire incident. For this purpose, the biomass combustion model suggested by European Monitoring and Evaluation Program (EMEP), 2019 was used (Bilgiç et al., 2021). According to that model, emitted dry mass can be estimated using the following equation:

$$M = A * B * \alpha * \beta$$

Where,

M – dry mass emitted

B – burned biomass amount

A – burned biomass area

β – burning efficiency of above ground biomass

α – fraction of above-average above-ground biomass

3.11.1 EMISSIONS ESTIMATION PROCESS:

Each of the components of the fuel classes are attributed a specific burning efficiency and emission factor for gas-phase or aerosol compounds, dependent also on the fire flaming or smoldering which is related with the diameter of the fuel type. Emission factors for CO, CH₄, VOC, NO_x, N₂O and SO₂ are taken from literature. If no local data on aboveground fuel load is available, default values can be applied. Values of total biomass for five biomes (boreal forest, temperate forest, Mediterranean forest, shrub land, grassland/steppe) and factors for each biome allowing aboveground biomass and the assumed fraction of biomass burnt in a fire to be derived, are provided. Biomass is converted into carbon by the multiplication with 0.45. The burning efficiency depends on the meteorological conditions and determines the type of combustion which may lead to flaming or smoldering fires. Depending on the available data, the above factors can be computed with more or less detail (Shahid et al., 2019).

Burnt areas may be available as a geographic layer or as a global value for a country or a region. In the case of geographic information, the type of vegetation burnt by the fire can eventually be divided according to fuel type, if this layer is available. If no local data on aboveground fuel load is available, default values can be applied. In the case of available geographical information of the burnt areas, the pre-fire vegetation can be classified into fuel types and distinctive fuel loads can be used for estimating emissions. In most ecosystems, there is currently hardly any information on fuel load. In particular, the classification of fuel into compartments showing various susceptibilities in a fire event is lacking. The latter is essential in the determination of fuel consumption — being the fraction of fuel actually consumed in a fire — as well as the fuel load fractions burning under smoldering or flaming combustion conditions and thus determining the species composition of the emissions (Chowdhury et al., 2013).

CHAPTER 4: RESULTS AND DISCUSSIONS

4.1 LOW-COST SENSOR NETWORK:

Low-cost sensor network was strategically established specifically in twin cities, Islamabad and Rawalpindi to develop a robust air quality profile of both the cities around the year. This network was established as part of a US State Department project lead by Duke University titled as, “Building Capacity to Improve Air Quality in South Asia: Reducing PM_{2.5} Through Low-Cost Sensor Network Driven Policy Decisions”. Around 30-35 low-cost sensors were deployed around the strategic public and private locations in twin cities building a through network providing with integrated real-time data of air quality. The network of these LCS across Pakistan and in twin cities is shown below:

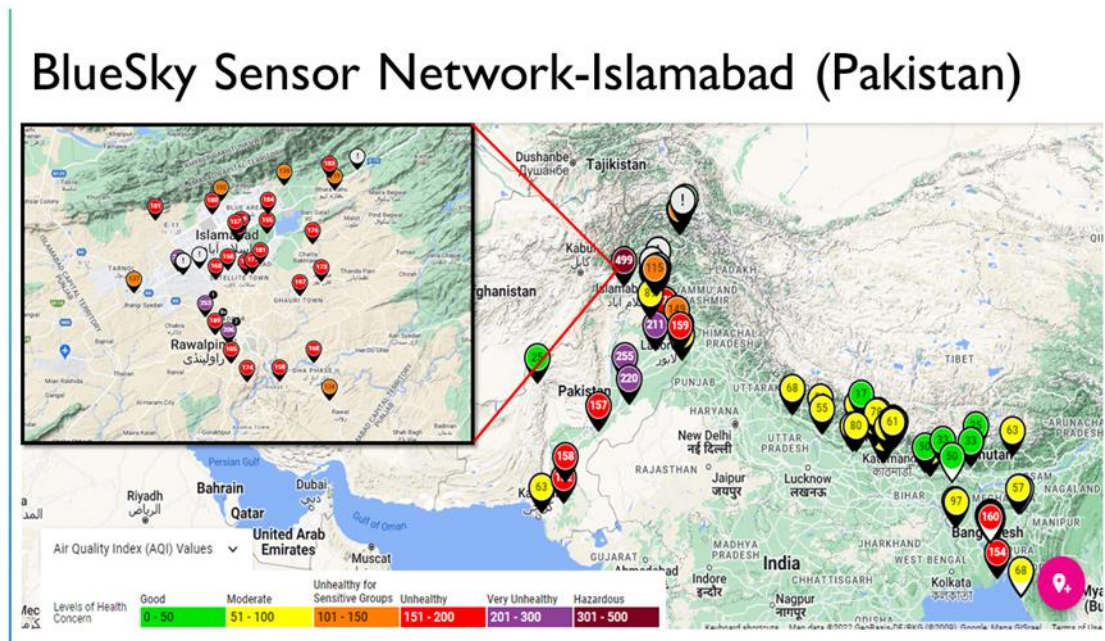


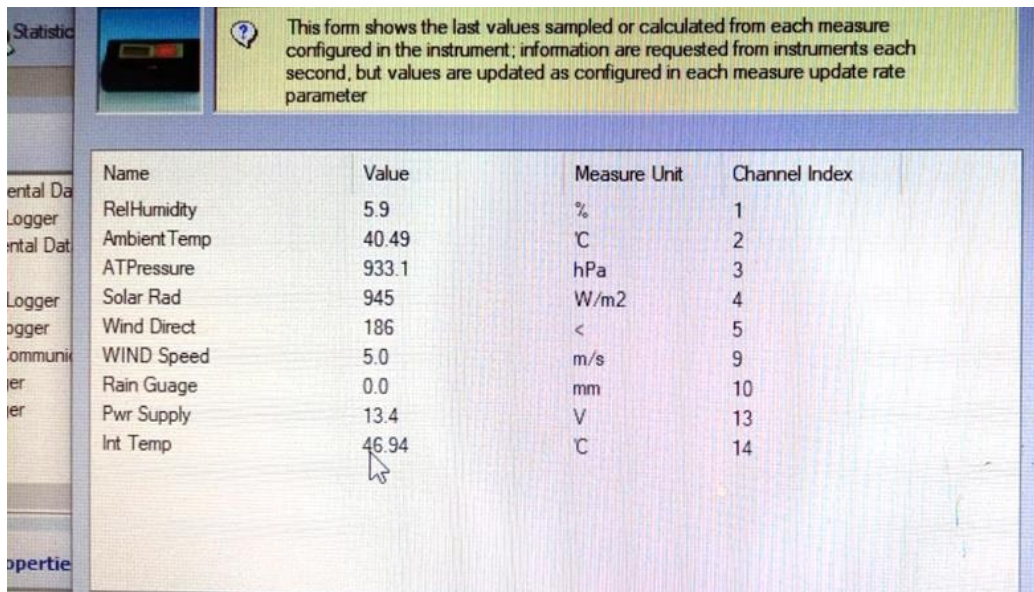
Figure 4. 1 TSI BlueSky low-cost sensor network in Islamabad and Rawalpindi against the installations all over Pakistan

4.2 FIRE EVENT IN NUST H-12:

On the afternoon of June 7, 2022, a conflagration erupted within the confines of the National University of Sciences and Technology (NUST) H-12 campus, initiating a sequence of events that posed significant challenges to emergency response efforts and environmental stability. The outbreak, originating within the campus precincts, swiftly

burgeoned, owing to the abundant presence of combustible biomass material within the vicinity.

Over the ensuing period of approximately 3 to 4 hours, the blaze propagated throughout the campus perimeter, engendering widespread devastation and infrastructural damage. Critical to the dynamics of the event were meteorological factors, notably the prevailing wind conditions. Recorded observations indicated a northeasterly wind direction, corresponding to 186 degrees on the cardinal compass, with a measured speed of 2.6 meters per second, translating to approximately 9.36 kilometers per hour. The interplay between wind direction and velocity exerted a pronounced influence on the fire's behavior, facilitating its rapid spread and altering its trajectory. The southern airflow served as a vector, guiding the propagation of flames across the campus terrain. Concurrently, the modest wind speed, though relatively subdued, nonetheless contributed to the acceleration and diffusion of the fire front.



This form shows the last values sampled or calculated from each measure configured in the instrument; information are requested from instruments each second, but values are updated as configured in each measure update rate parameter

Name	Value	Measure Unit	Channel Index
RelHumidity	5.9	%	1
Ambient Temp	40.49	°C	2
ATPressure	933.1	hPa	3
Solar Rad	945	W/m ²	4
Wind Direct	186	°	5
WIND Speed	5.0	m/s	9
Rain Guage	0.0	mm	10
Pwr Supply	13.4	V	13
Int Temp	46.94	°C	14

Figure 4. 2 User interface of software to observe meteorological parameters through weather station installed at IESE, NUST

In response to the exigency, emergency responders and firefighting contingents mobilized promptly to mitigate the escalating crisis. Their coordinated intervention, characterized by strategic resource allocation and tactical deployment, culminated in the successful containment and extinguishment of the inferno. Despite the formidable challenges posed

by adverse meteorological conditions and logistical constraints, their concerted efforts yielded a favorable outcome, averting further cataclysmic ramifications. Subsequent to the containment phase, the affected community rallied in solidarity, demonstrating resilience and cohesion in the aftermath of the calamitous event. Despite the deleterious impact wrought upon the NUST H-12 campus and its environs, the collective response underscored the capacity for collaborative action and adaptive resilience in confronting and surmounting adversarial circumstances.

4.3 SATELLITE VS BLUESKY SENSOR OBSERVATIONS:

During the wildfire event under investigation, two Bluesky low-cost air quality monitoring sensors, denoted as NUST Pk-3 and NUST Pk-6, were deployed at strategic locations within the NUST campus. These sensors were selected for their affordability, portability, and ability to provide real-time measurements of key air pollutants, including particulate matter (PM_{2.5}). Upon scrutinizing the data acquired from the deployed sensors, a conspicuous pattern emerged, revealing a sharp spike in PM_{2.5} concentration coinciding precisely with the onset of the wildfire. This sudden increase in particulate matter concentration, as evidenced by both NUST Pk-3 and NUST Pk-6 sensors, provides empirical validation of the wildfire event and its deleterious impact on local air quality.

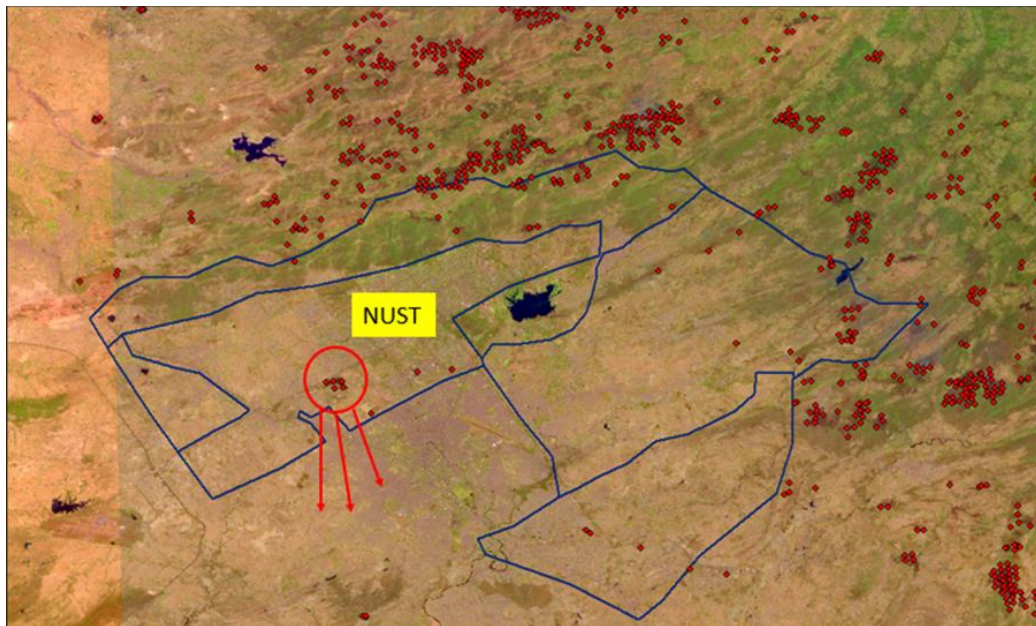


Figure 4. 3 Sentinel 2-A 20m x 20m RGB image and VIIRS active fire hotspot MODIS products verifying active burning site in NUST H-12 Campus on 8th June, 2022

4.4 DISCUSSION:

The integration of satellite imagery and ground-based sensor data offers a synergistic approach to wildfire monitoring and assessment. By corroborating satellite-derived fire hotspots with ground-truth observations of PM_{2.5} concentration, this study presents a robust framework for understanding the spatiotemporal dynamics of wildfires and their associated environmental ramifications. Moreover, the utilization of low-cost air quality sensors demonstrates their utility as cost-effective tools for monitoring air pollution in real-time, particularly during natural disasters such as wildfires. The amalgamation of satellite imaging and ground-based sensor data yields valuable insights into the multifaceted aspects of wildfire events. This interdisciplinary approach enhances our ability to accurately detect, monitor, and assess the impact of wildfires on both terrestrial and atmospheric ecosystems.

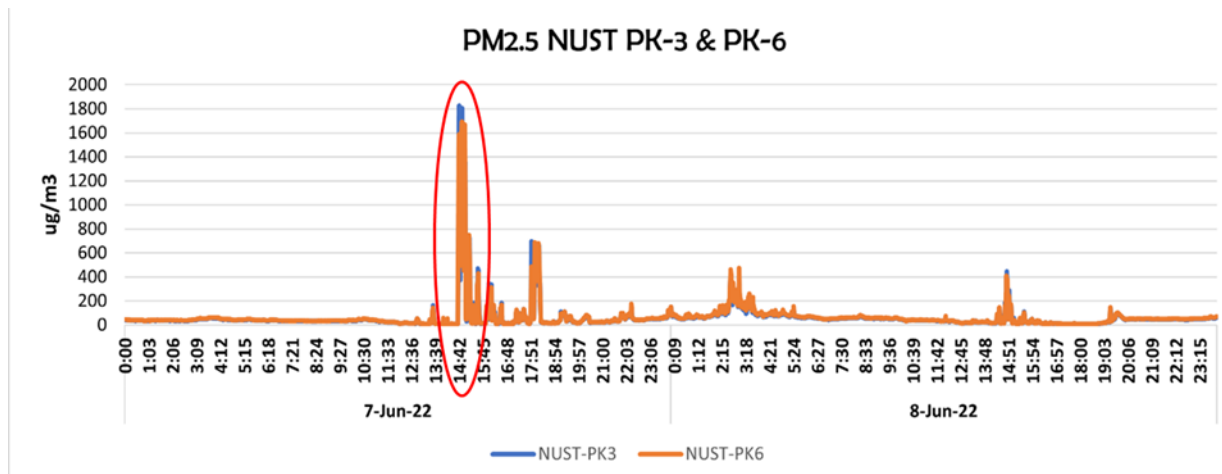


Figure 4. 4 TSI BlueSky sensors NUST Pk-3 and NUST Pk-6 installed at IESE, NUST response to fire on 7th June, 2022

4.5 ABOVE GROUND BIOMASS (AGB) / BURNT BIOMASS:

Aboveground biomass states the total mass of living plant material found above the soil surface within a given area or ecosystem. This biomass encompasses various components of plants, including stems, branches, leaves, flowers, fruits, and any other aboveground structures. It is an important measure in ecology and forestry, providing insights into the productivity, carbon storage, and overall health of terrestrial ecosystems. Scientists often quantify aboveground biomass to understand the distribution and dynamics of plant communities, assess ecosystem productivity, estimate carbon sequestration potential, and monitor changes in vegetation over time. This measurement is typically conducted using

field sampling methods such as harvesting and weighing plant components, or through remote sensing techniques like satellite imagery and Light Detection and Ranging (LiDAR) technology.

The fraction of above-average above-ground biomass and burned biomass amount were taken as suggested by EMEP/EEA, 2019

Table 4. 1 Above-average above-ground biomass (α) and burned biomass amount (B) constants by EMEP/EEA, 2019

	Mixed forest	Scrubland	Temperate Forest	Mediterranean forest	Steppe (Grassland)
B	20	7.5	35	15	2
α	0.75	0.64	0.75	0.75	0.35

BURN SEVERITY:

Burn severity describes how the fire intensity affects the functioning of the ecosystem in the area that has been burnt. The observed effects often vary within the area and between different ecosystems. We obtained the β values for each level of burn severity from the EMEP/EEA (2019) data. This resource provides valuable information on burning efficiency, which is expressed as a percentage, for different types of vegetation, such as temperate forests, Mediterranean forests, scrubland, and grassland. According to EMEP/EEA (2019), the burning efficiency is estimated to be 0.20, 0.25, 0.50, and 0.50 for these vegetation types, respectively. To determine the weighted averages of the burning efficiency based on the burn severity, we used the β values and calculated the averages for forests and scrubland. Specifically, we calculated the weighted average burning efficiency for forests to be 0.25 and for scrubland to be 0.52. This information is important for assessing the environmental impact of the fire and for designing appropriate management strategies to mitigate any negative effects.

Table 4. 2 Burn severity (β) constants for forests and scrubland suggested by EMEP/EEA 2019

β (Burn Severity)	Burn Efficiencies	
	Scrubland (Steppes)	Forests
Low	0.25	0.05
Low (Moderate)	0.50	0.25
High (Moderate)	0.75	0.30
High	1.00	0.50
Average (Weighted)	0.52	0.25

4.6 EMISSION ESTIMATION:

As per the guideline book of EEA/EMEP 2019, the emission calculations due to forest fires can be done with a number of methods divided into tiers based on the extent of information available. Based on our scenario, we tend to go with tier 2 methodology, which includes calculating the emission in two steps:

- estimate the emissions of carbon from the burned land;
- estimate the emissions of other trace gases using emission ratios with respect to carbon

For the first step, we calculated the total burned dry mass, by using the equation mentioned above. Then we multiplied it with the factor 0.45 as previously mentioned to estimate the value of burned carbon. The equation for estimation of carbon mass is given as:

$$C = 0.45 (M)$$

These calculation for a number of burnt sites around Islamabad Capital territory are given as follows:

Table 4. 3 Location-wise burned area, emitted dry mass and carbon mass using biomass combustion model

Fire Location	Area(m ²)	Area (km ²)	Emitted Dry Mass(M) kg/m ²	Carbon Mass (C) kg/m ²
NUST	656755	0.656755	1639260.48	737667.216
Margalla Hills	19597948	19.59795	48916478.21	22012415.19
Karore	33696784	33.69678	84107172.86	37848227.79
Ayubia	677667	0.677667	1691456.832	761155.5744
Khanpur	2612152	2.612152	6519931.392	2933969.126

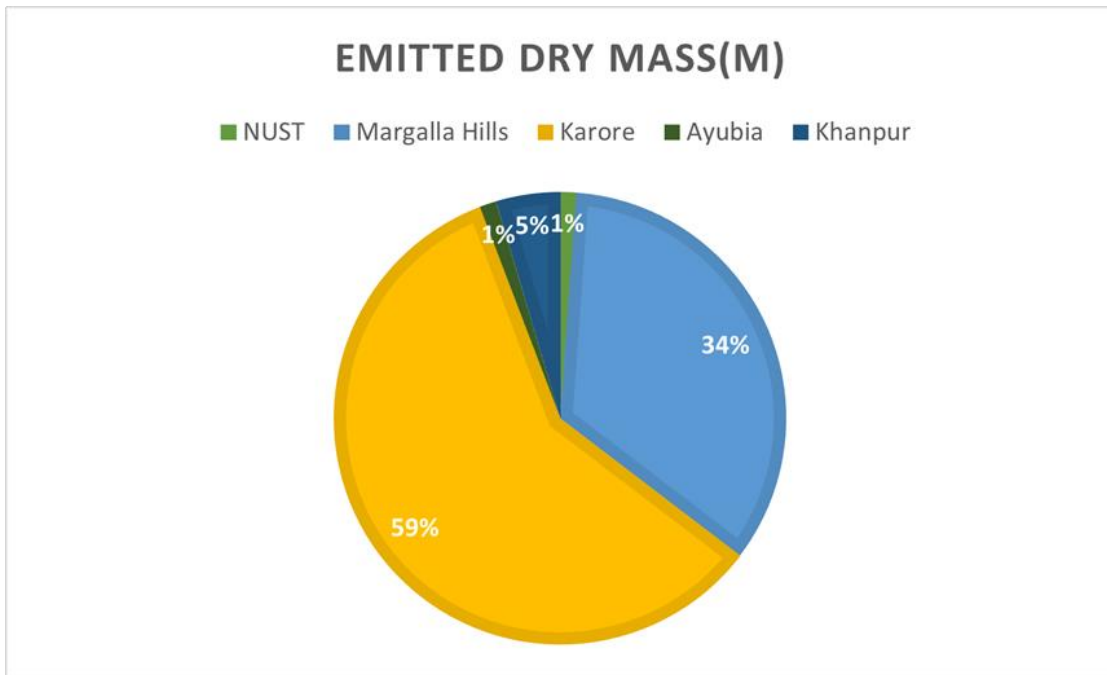


Figure 4. 5 Pie-chart distribution of emitted dry mass concentration relevant to the respective location

4.6.1 CONVERSION FACTORS:

The emission of any particular species can then be obtained by multiplying the mass of carbon formed by the emission ratios (in g/kg C) which is given as follows:

Table 4. 4 Conversion factor for each pollutant as suggested by EMEP/EEA 2019

Pollutant(s)	Conversion Factor	Unit(s)
NO _x	8.0	g/kg C (emitted)
CO	230.0	g/kg C (emitted)
SO ₂	1.60	g/kg C (emitted)
TSP	17.0	g/kg wood burned
PM ₁₀	11.0	g/kg wood burned
PM _{2.5}	9.0	g/kg wood burned
Black Carbon	9.0	%age of PM _{2.5}

4.6.2 EMISSIONS AT NUST:

Based on the above given equations and constants, the emissions at NUST were calculated as:

Table 4. 5 Concentration of each pollutant in NUST using emission factor by EMEP/EEA 2019

Pollutant	Emission Factors	Emissions (g/m ²)	Emissions (kg/ha)
NO _x	8	5901337.728	590.1338
CO	230	169663459.7	16966.35
SO ₂	1.6	1180267.546	118.0268
TSP	17	12540342.67	1254.034
PM ₁₀	11	8114339.376	811.4339
PM _{2.5}	9	6639004.944	663.9005
BC	9	597510.445	59.75104
CH ₄	15	11065008.24	1106.501
NH ₃	1.8	1327800.989	132.7801

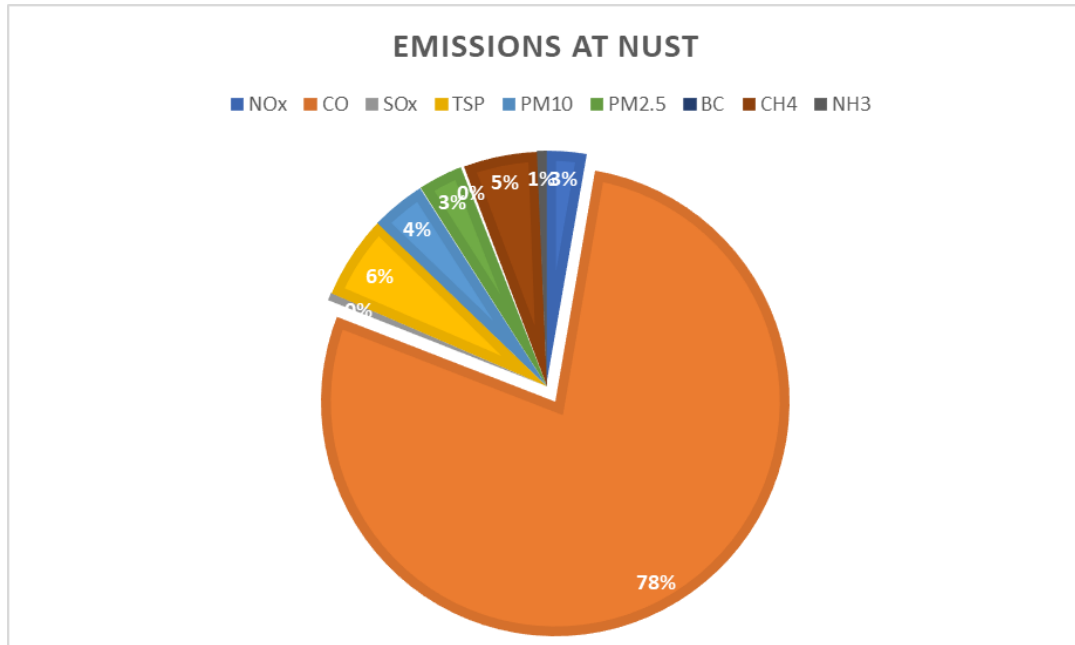


Figure 4. 6 Pie-chart distribution of concentration of each pollutant at NUST H-12 Campus

4.6.3 EMISSIONS AT MARGALLA HILLS:

Margalla Hills suffered highest amount of forest and bushfires in 2022 covering a vast land area from ICT to Khyber Pakhtunkhwa. Large masses of trees and bushes were burnt. These fires had a massive impact on local residents too as apart from gaseous emissions, they added tons of ash in the breathing environment of every living being in the surrounding areas. The areas largely impacted by the fires are shown below:

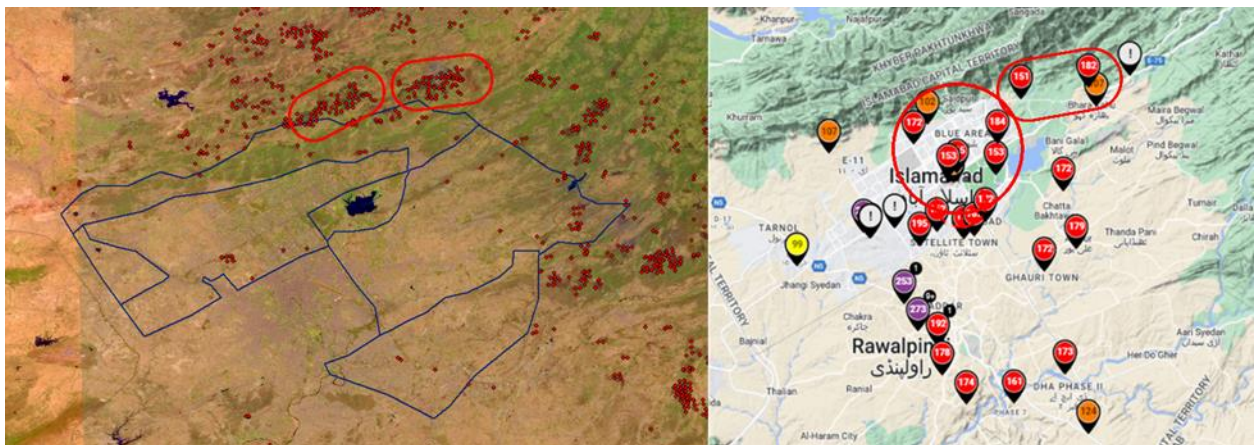


Figure 4. 7 Comparison of Sentinel 2-A RGB image against VIIRS fire hotspot products against TSI BlueSky sensors' increased concentration

The calculated emissions at Margalla Hills as per the given conversion factors are as follows:

Table 4. 6 Concentration of each pollutant in Margalla Hill sites using emission factor by EMEP/EEA 2019

Pollutants	Emission (g/m2)	Margalla (kg/ha)
NOx	176099321.5	17609.93215
CO	5062855495	506285.5495
SO ₂	35219864.31	3521.986431
TSP	374211058.3	37421.10583
PM ₁₀	242136567.1	24213.65671
PM _{2.5}	198111736.7	19811.17367
BC	198111736.7	19811.17367
CH ₄	330186227.9	33018.62279
NH ₃	39622347.35	3962.234735

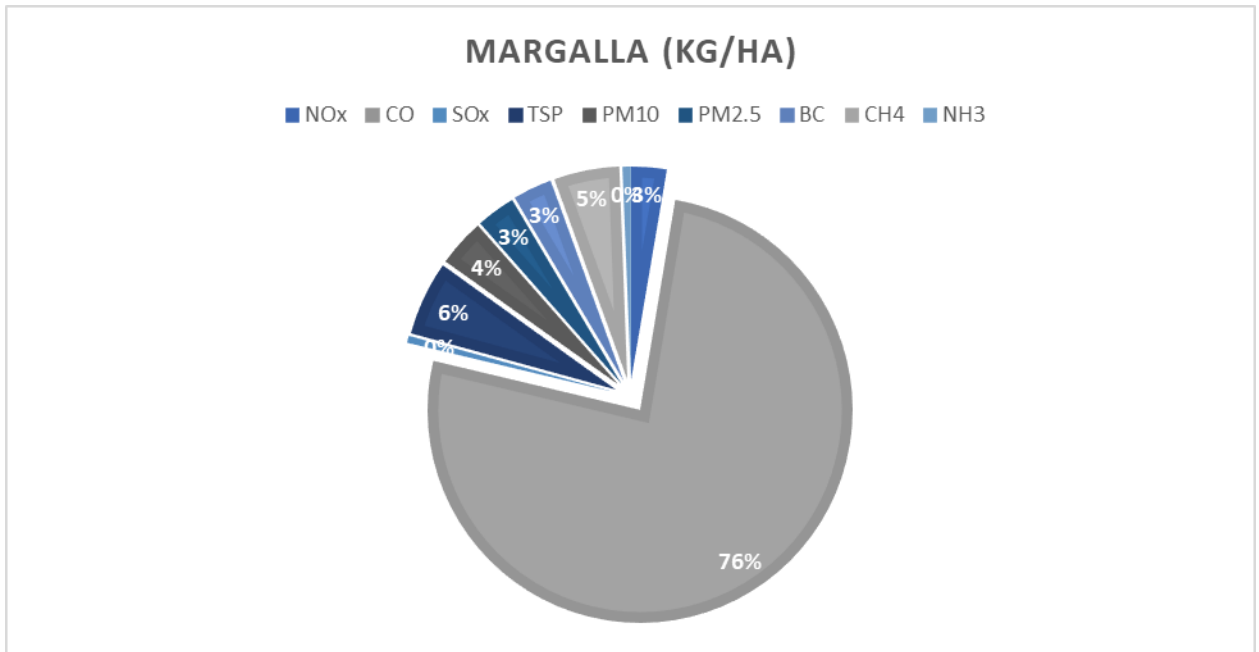


Figure 4. 8 Pie-chart distribution of concentration of each pollutant at Margalla Hills

4.6.4 EMISSIONS IN KARORE VILLAGE:

Located on the southwestern periphery of Kotli Sattian, the village of Karor stands as a prominent settlement, notable for its proximity to the capital city of Islamabad. Spanning an area of approximately 3,001 acres, Karor is situated at a distance of approximately 22 kilometers from Kotli Sattian, with accessibility facilitated by well-developed metallic roads traversing its periphery. The fertile soil of the village lends itself to the cultivation of local crops; however, the socio-economic landscape of Karor is shaped by a prevailing trend of inhabitants seeking employment opportunities in urban centers.

Despite the agricultural potential inherent to the village, a notable proportion of Karor's populace has opted for temporary migration to metropolitan areas, drawn by the allure of modern amenities and enhanced educational prospects for their progeny. It is estimated that forty percent of the village's population has embarked upon this migration, reflecting a broader societal transition towards urbanization and the pursuit of socio-economic advancement beyond traditional agrarian livelihoods. Being densely surrounded by bushes and forests, Karore and its surroundings also faced a lot of active bushfires in 2022, which although did not cause any life and property damage yet caused severe health implications on both humans and livestock animals. Heavy ash clouds swerved over the village as fire and embers kindled for more than 3 days around it.

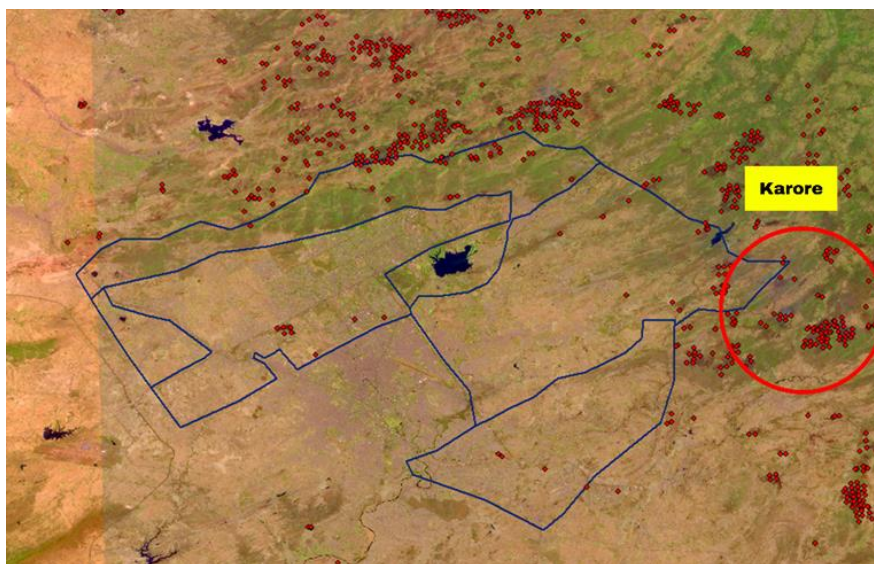


Figure 4. 9 Active burning sites around Karore village verified by VIIRS fire hotspot product and Sentinel 2-A RGB image

The calculated emissions at Karore Village as per the given conversion factors are as follows:

Table 4. 7 Concentration of each pollutant in Karore Village using emission factor by EMEP/EEA 2019

Pollutants	Emission Karore (g/m ²)	Karore (kg/ha)
NO _x	302785822.3	30278.58223
CO	8705092391	870509.2391
SO ₂	60557164.46	6055.716446
TSP	643419872.4	64341.98724
PM ₁₀	416330505.7	41633.05057
PM _{2.5}	340634050.1	34063.40501
BC	340634050.1	34063.40501
CH ₄	567723416.8	56772.34168
NH ₃	68126810.02	6812.681002

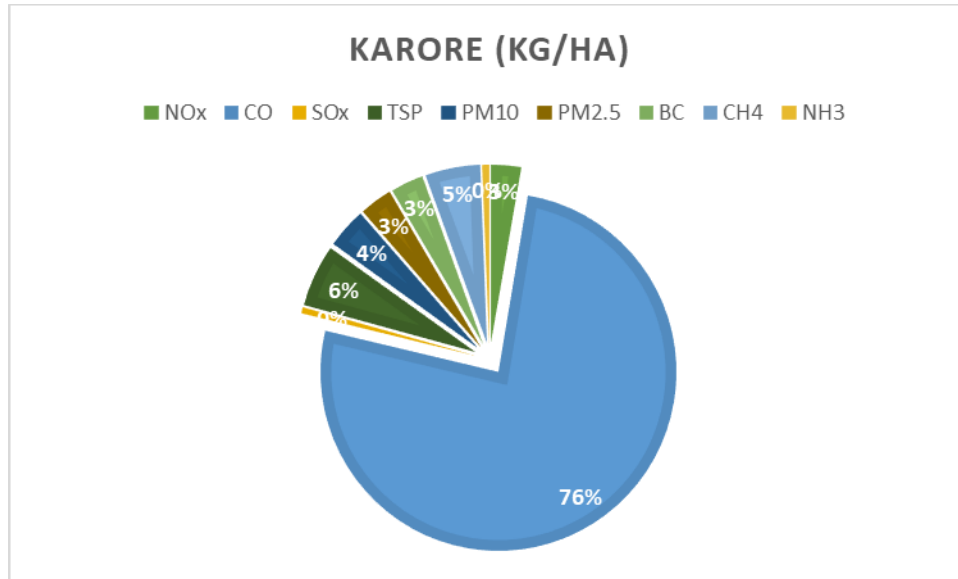


Figure 4. 10 Pie-chart distribution of concentration of each pollutant at Karore Village

4.6.5 EMISSIONS IN PATRIATA:

Patriata, colloquially referred to as New Murree, embodies a quintessential hill station nestled amidst the northern expanse of Punjab, Pakistan. Positioned approximately 15 kilometers southeast of the iconic Murree hill, Patriata finds its abode within the administrative jurisdiction of Murree Tehsil, a subdivision of Murree District.

Distinguished by its lofty altitude, Patriata claims the highest elevation in its environs, with the surrounding hills soaring to a majestic height of 7,500 feet above sea level.

Renowned for its temperate climate, Patriata beckons travelers seeking respite from the sweltering heat prevalent in more southerly regions. Patriata's topography is characterized by dense vegetation, with lush forests enveloping the area in verdant splendor.

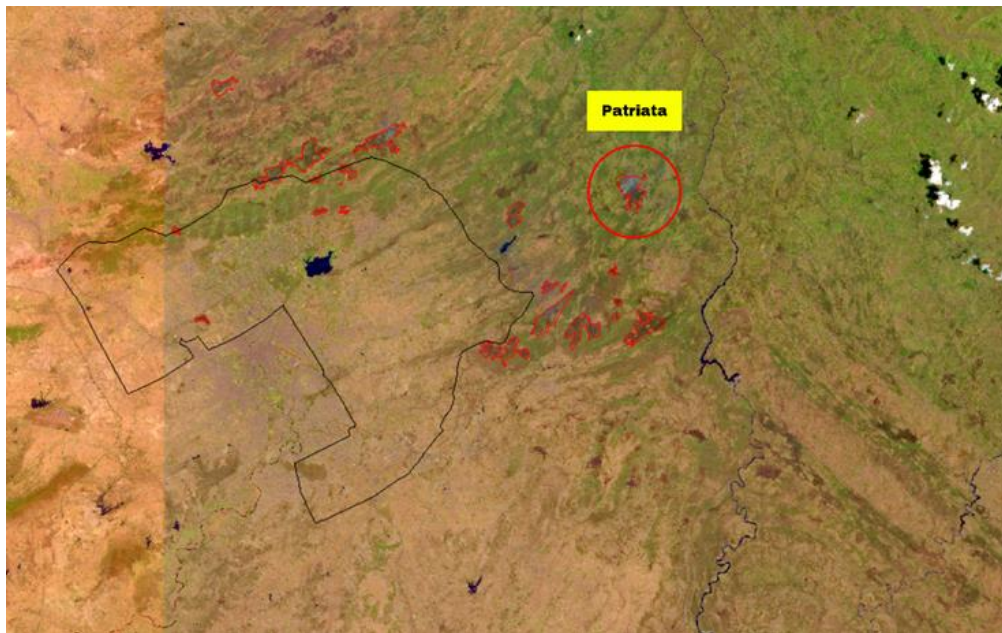


Figure 4. 11 Active burning sites around Patriata verified by VIIRS fire hotspot product and Sentinel 2-A RGB image

The calculated emissions at Patriata Hills as per the given conversion factors are as follows:

Table 4. 8 Concentration of each pollutant in Patriata using emission factor by EMEP/EEA 2019

Pollutants	Emission Patriata (g/m2)	Patriata (kg/ha)
NOx	6089244.595	608.9244595
CO	175065782.1	17506.57821
SO ₂	1217848.919	121.7848919
TSP	12939644.76	1293.964476
PM ₁₀	8372711.318	837.2711318
PM _{2.5}	6850400.17	685.040017
BC	6850400.17	685.040017
CH ₄	11417333.62	1141.733362
NH ₃	1370080.034	137.0080034

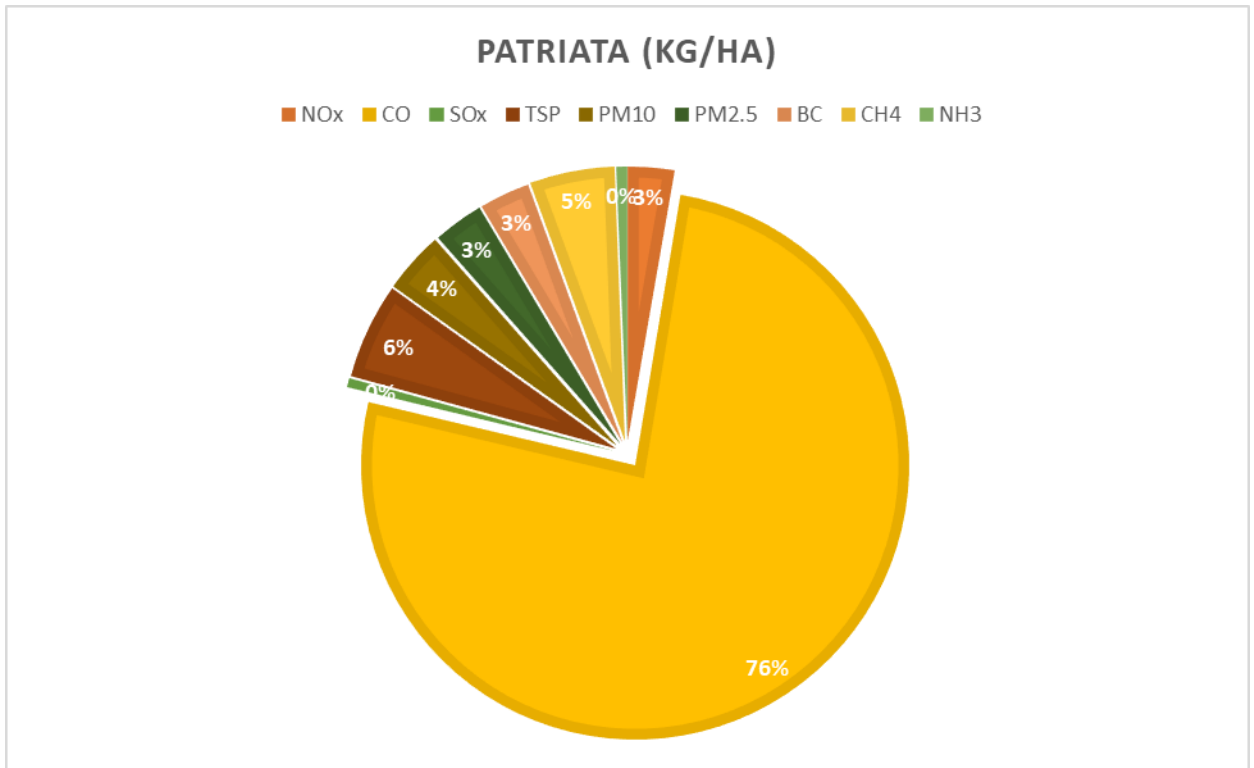


Figure 4. 12 Pie-chart distribution of concentration of each pollutant at Patriata

CHAPTER 5: CONCLUSIONS AND FUTURE RECOMMENDATION

5.1 CONCLUSIONS:

This study was carried out with two objectives pushing towards the same goal of designing a robust tech-integrated air quality monitoring system to develop a strong database for guided policy decisions. The area selected was in and around twin cities of Islamabad and Rawalpindi. Around 36 low-cost air quality monitoring sensors (by TSI BlueSky) were deployed at strategic locations in both the cities including urban, semi-urban and rural areas which also included forest covers.

In terms of integrating low-cost sensors with solar, following conclusions can be drawn from the observations:

- Low-cost air quality monitoring sensors can prove to be quite a resourceful tool to develop air quality profile of any city in Pakistan.
- Solar powered backup has been a beneficial alternative for the power and internet source for low-cost sensors.
- Developing a robust self-powered solar-based strategic network of air quality sensors in any big city of Pakistan would primarily consist of around 50 sensors and would cost somewhere around PkR 1 million.
- Fire events in Islamabad Capital Territory in 2022 were largely caused by prolonged extremely high temperature and dry weather. Consequently, these fires have affected large portions of forest covers in Islamabad close to the urban settlement making the surrounding air polluted and unbreathable.
- Emissions estimation shows an overall similar emission profile across all the burnt sites in and around Islamabad.
- It is evident that all the harmful gases and particulates were emitted as result of this fire in the area. The emissions included not only carbon dioxide (CO₂) but also large portions of carbon monoxide (CO), methane (CH₄), PM_{2.5} & PM₁₀, ammonia (NH₃), oxides of nitrogen (NO_x), oxides of sulfur (SO_x), and black carbon (BC).
- While considering fire site in NUST, almost 664kg/ha and 811kg/ha of PM_{2.5} and PM₁₀ were emitted respectively. Carbon monoxide emission here was around

16966kg/ha while methane emission was around 1106kg/ha. The total carbon mass estimated through this model on NUST site was approximately 73.7kg/ha.

- In Margalla Hills sites, PM_{2.5} and PM₁₀ are 19,811kg/ha and 24,213kg/ha respectively. Carbon monoxide (CO) concentration at these sites was also higher compared to other pollutants standing at 506,285.55kg/ha.
- Similarly in Karore village, which is surrounded by bushes and forests, PM_{2.5} and PM₁₀ values are observed as 34,063kg/ha and 41,633kg/ha respectively. Here carbon monoxide (CO) value stands at a high 870,509kg/ha.
- Results show that carbon monoxide is present in large concentrations at all sites unanimously, which may be due to following reasons:
- Incomplete Combustion: Biomass burning often occurs under conditions of incomplete combustion, leading to the release of elevated levels of carbon monoxide.
- High Carbon Content: Biomass materials, such as wood, crop residues, and vegetation, contain high levels of carbon. During burning, this carbon is released into the atmosphere in the form of carbon monoxide, contributing to elevated CO concentrations.
- Atmospheric Conditions: Meteorological factors, such as temperature inversions and stagnant air masses, can exacerbate the accumulation of pollutants, including carbon monoxide, around biomass burning sites.
- Biomass Type and Composition: Different types of biomass materials exhibit varying combustion characteristics and CO emission potentials. For example, the combustion of wet or green biomass tends to produce higher levels of carbon monoxide
- Scale and Intensity of Burning: The scale and intensity of biomass burning activities influence the magnitude of CO emissions. Large-scale biomass burning events, such as forest fires or agricultural field burning, can release substantial quantities of carbon monoxide into the atmosphere, especially if the burning is prolonged or uncontrolled.

The most relevant reason in the current available scenario is high carbon content in the forests and bushes of Margalla Hills. The burning this high carbon content with humidity present in the air results in large amounts of carbon monoxide production apart from other pollutants.

5.2 RECOMMENDATIONS:

Based on the results and outcomes of this study, the innovations and interventions that can be done in the system are quite evident. Some of the key recommendations are given as follows:

- Low-cost sensors should be incorporated into the mainstream urban infrastructure to keep a real time and thorough profiles of air quality of any urban settlement in Pakistan.
- Integration of solar panel with low-cost sensors proved to be a fruitful amalgam of technology. If done at a larger and commercial scale, this solution will enable the air quality sensors to be deployed in far off remote areas with no availability of electricity or Wifi.
- Research and development in air quality monitoring and control should be encouraged and promoted in public and private sectors at all scales. National and international funds should be mobilized by private entities to support a robust research-based framework on air quality control.
- Apart from IoT, machine learning, data processing and artificial intelligence tools should be introduced and utilized in air quality monitoring and control to assist the policy makers in having a clear view of state of air quality of all major cities of Pakistan.
- Capacity building should be done at policy making level to help the government sector comprehend swiftly evolving technologies and how to benefit from them while developing a policy action roadmap.
- Bushfire and forest fire events pose a serious threat not only to the health and well-being of people, but also of the ecosystem and the natural habitat of native species. Consequently, measures should be taken to quickly respond to such situations in future to limit the burning and thus amount of harmful emissions.

REFERENCES

- Al-Hasn, R., & Almuhammad, R. (2022). Burned area determination using Sentinel-2 satellite images and the impact of fire on the availability of soil nutrients in Syria. *Journal of Forest Science*, 68(3), 96–106. <https://doi.org/10.17221/122/2021-JFS>
- Badura, M., Sówka, I., Batog, P., Szymański, P., & Dabrowski, L. (2019). Sensor network for PM2.5 measurements on an academic campus area. *E3S Web of Conferences*, 116. <https://doi.org/10.1051/e3sconf/201911600004>
- Bilal, M., Mhawish, A., Nichol, J. E., Qiu, Z., Nazeer, M., Ali, M. A., de Leeuw, G., Levy, R. C., Wang, Y., Chen, Y., Wang, L., Shi, Y., Bleiweiss, M. P., Mazhar, U., Atique, L., & Ke, S. (2021). Air pollution scenario over Pakistan: Characterization and ranking of extremely polluted cities using long-term concentrations of aerosols and trace gases. *Remote Sensing of Environment*, 264. <https://doi.org/10.1016/j.rse.2021.112617>
- Bilgiç, E., Tuygun, G. T., & Gunduz, O. (2021). *Determination of Air Pollution from Wildfires with Satellite Observations Assessment of Seasonal and Annual Fluctuations of Groundwater Storage □ Based-on The Gravity Recovery and Climate Experiment (GRACE) Measurements View project TÜBİTAK 119Y005 View project*. <https://www.researchgate.net/publication/356791231>
- Bonyadi, Z., Arfaeinia, H., Fouladvand, M., Farjadfard, S., Omidvar, M., & Ramavandi, B. (2021). Impact of exposure to ambient air pollutants on the admission rate of hospitals for asthma disease in Shiraz, southern Iran. *Chemosphere*, 262. <https://doi.org/10.1016/j.chemosphere.2020.128091>
- CCRD. (2022).
- Chowdhury, Z., Campanella, L., Gray, C., Al Masud, A., Marter-Kenyon, J., Pennise, D., Charron, D., & Zuzhang, X. (2013). Measurement and modeling of indoor air pollution in rural households with multiple stove interventions in Yunnan, China. *Atmospheric Environment*, 67, 161–169. <https://doi.org/10.1016/j.atmosenv.2012.10.041>
- Chu, H. J., Ali, M. Z., & He, Y. C. (2020). Spatial calibration and PM2.5 mapping of low-cost air quality sensors. *Scientific Reports*, 10(1). <https://doi.org/10.1038/s41598-020-79064-w>
- Coudray, N., Dieterlen, A., Roth, E., & Trouvé, G. (2009). Density measurement of fine aerosol fractions from wood combustion sources using ELPI distributions and image processing techniques. *Fuel*, 88(5), 947–954. <https://doi.org/10.1016/j.fuel.2008.12.013>
- Hosseini, S., Li, Q., Cocker, D., Weise, D., Miller, A., Shrivastava, M., Miller, J. W., Mahalingam, S., Princevac, M., & Jung, H. (2010). Particle size distributions from laboratory-scale biomass fires using fast response instruments. *Atmospheric Chemistry and Physics*, 10(16), 8065–8076. <https://doi.org/10.5194/acp-10-8065-2010>
- Jiang, R., & Bell, M. L. (2008). A comparison of particulate matter from biomass-burning rural and non-biomass-burning urban households in northeastern China. *Environmental Health Perspectives*, 116(7), 907–914. <https://doi.org/10.1289/ehp.10622>
- Li, J., Zhang, H., Chao, C. Y., Chien, C. H., Wu, C. Y., Luo, C. H., Chen, L. J., & Biswas, P. (2020). Integrating low-cost air quality sensor networks with fixed and satellite monitoring systems to

- study ground-level PM2.5. *Atmospheric Environment*, 223. <https://doi.org/10.1016/j.atmosenv.2020.117293>
- Liang, L. (2021). Calibrating low-cost sensors for ambient air monitoring: Techniques, trends, and challenges. In *Environmental Research* (Vol. 197). Academic Press Inc. <https://doi.org/10.1016/j.envres.2021.111163>
- Lin, L., Li, X., & Gu, W. (2017). PM2.5 monitoring system based on ZigBee wireless sensor network. *IOP Conference Series: Earth and Environmental Science*, 69(1). <https://doi.org/10.1088/1755-1315/69/1/012094>
- Lu, Y., Giuliano, G., & Habre, R. (2021). Estimating hourly PM2.5 concentrations at the neighborhood scale using a low-cost air sensor network: A Los Angeles case study. *Environmental Research*, 195. <https://doi.org/10.1016/j.envres.2020.110653>
- Manisalidis, I., Stavropoulou, E., Stavropoulos, A., & Bezirtzoglou, E. (2020). Environmental and Health Impacts of Air Pollution: A Review. In *Frontiers in Public Health* (Vol. 8). Frontiers Media S.A. <https://doi.org/10.3389/fpubh.2020.00014>
- Metia, S., Nguyen, H. A. D., & Ha, Q. P. (2021). IoT-enabled wireless sensor networks for air pollution monitoring with extended fractional-order kalman filtering. *Sensors*, 21(16). <https://doi.org/10.3390/s21165313>
- Mir, K. A., Purohit, P., Cail, S., & Kim, S. (2022). Co-benefits of air pollution control and climate change mitigation strategies in Pakistan. *Environmental Science and Policy*, 133, 31–43. <https://doi.org/10.1016/j.envsci.2022.03.008>
- Norovsuren, B., Tseveen, B., Batomunkuev, V., & Renchin, T. (2019). Estimation for forest biomass and coverage using Satellite data in small scale area, Mongolia. *IOP Conference Series: Earth and Environmental Science*, 320(1). <https://doi.org/10.1088/1755-1315/320/1/012019>
- Orach, J., Rider, C. F., & Carlsten, C. (2021). Concentration-dependent health effects of air pollution in controlled human exposures. In *Environment International* (Vol. 150). Elsevier Ltd. <https://doi.org/10.1016/j.envint.2021.106424>
- Prado, G. F., Zanetta, D. M. T., Arbex, M. A., Braga, A. L., Pereira, L. A. A., de Marchi, M. R. R., de Melo Loureiro, A. P., Marcourakis, T., Sugauara, L. E., Gattás, G. J. F., Gonçalves, F. T., Salge, J. M., Terra-Filho, M., & de Paula Santos, U. (2012). Burnt sugarcane harvesting: Particulate matter exposure and the effects on lung function, oxidative stress, and urinary 1-hydroxypyrene. *Science of the Total Environment*, 437, 200–208. <https://doi.org/10.1016/j.scitotenv.2012.07.069>
- Rasheed, A., Aneja, V. P., Aiyyer, A., & Rafique, U. (2014). Measurements and analysis of air quality in Islamabad, Pakistan. *Earth's Future*, 2(6), 303–314. <https://doi.org/10.1002/2013ef000174>
- Rasheed, A., Aneja, V. P., Aiyyer, A., & Rafique, U. (2015). Measurement and analysis of fine particulate matter (PM2.5) in urban areas of Pakistan. *Aerosol and Air Quality Research*, 15(2), 426–439. <https://doi.org/10.4209/aaqr.2014.10.0269>
- Government of Pakistan, & Ministry of Planning, D. and S. I. I. (2022). *RESILIENT RECOVERY, REHABILITATION, AND RECONSTRUCTION FRAMEWORK PAKISTAN (4RF)* Government of Pakistan Ministry of Planning, Development and Special Initiatives Islamabad.

- Sahu, R., Dixit, K. K., Mishra, S., Kumar, P., Shukla, A. K., Sutaria, R., Tiwari, S., & Tripathi, S. N. (2020). Validation of low-cost sensors in measuring real-time PM10 concentrations at two sites in delhi national capital region. *Sensors (Switzerland)*, *20*(5). <https://doi.org/10.3390/s20051347>
- Shahid, I., Chishtie, F., Bulbul, G., Shahid, M. Z., Shafique, S., & Lodhi, A. (2019). State of air quality in twin cities of Pakistan: Islamabad and Rawalpindi. *Atmosfera*, *32*(1), 71–84. <https://doi.org/10.20937/ATM.2019.32.01.06>
- Tainio, M., Jovanovic Andersen, Z., Nieuwenhuijsen, M. J., Hu, L., de Nazelle, A., An, R., Garcia, L. M. T., Goenka, S., Zapata-Diomedes, B., Bull, F., & Sá, T. H. de. (2021). Air pollution, physical activity and health: A mapping review of the evidence. In *Environment International* (Vol. 147). Elsevier Ltd. <https://doi.org/10.1016/j.envint.2020.105954>
- Xie, Y., Wang, Y., Zhang, K., Dong, W., Lv, B., & Bai, Y. (2015). Daily Estimation of Ground-Level PM2.5 Concentrations over Beijing Using 3 km Resolution MODIS AOD. *Environmental Science and Technology*, *49*(20), 12280–12288. <https://doi.org/10.1021/acs.est.5b01413>
- Xing, Y. F., Xu, Y. H., Shi, M. H., & Lian, Y. X. (2016). The impact of PM2.5 on the human respiratory system. In *Journal of Thoracic Disease* (Vol. 8, Issue 1, pp. E69–E74). Pioneer Bioscience Publishing. <https://doi.org/10.3978/j.issn.2072-1439.2016.01.19>